

BULLETIN OF THE NATIONAL
INSTITUTE OF
INDUSTRIAL HEALTH

No. 6

1961

労働衛生研究所研究報告

第 6 号

昭和三十六年

THE NATIONAL INSTITUTE
OF INDUSTRIAL HEALTH

MINISTRY OF LABOUR

労働省労働衛生研究所

THE NATIONAL INSTITUTE OF
INDUSTRIAL HEALTH

Kizuki-Sumiyoshi, Kawasaki, Japan

EDITORIAL BOARD

MASAYOSHI YAMAGUCHI, *Editor-in-Chief*

HIROYUKI SAKABE, SHIGEO KOIKE

EXPERIMENTAL STUDY ON TOLUENE POISONING AND EFFECT OF TOLUENE UPON THE RECOVERY FROM BENZENE POISONING IN RATS

Hiromichi HASEGAWA and Mitsuo SATO

Browning¹⁾ has reported that toluene is regarded as less chronically toxic than benzene, which coincides well with the findings reported by El Masri²⁾ that toluene is mainly converted into the non-toxic hippuric acid. This inference has been ascertained by many investigators by observing microscopically the blood picture of animals received toluene except Ishizu⁴⁾ and Hirasawa⁵⁾ who observed some changes in blood picture.

In the study of toluene poisoning, Urata⁶⁾ observed that the administration of toluene does not show any effect on the process of recovery from benzene poisoning.

This paper describes the effect of toluene on the recovery from benzene poisoning and toluene poisoning itself.

METHODS

Catalase activity:

Catalase activity was measured by the method reported by Hasegawa and Sato⁷⁾ in the study of benzene poisoning.

The ratio of non-heme protein to total protein in erythrocytes endosoma:

The amount of non-heme protein and total protein were measured by the method described previously by Sato and Hasegawa⁸⁾ using a technique of column chromatography. The value of the ratio was computed by the following equation:

$$\left(\frac{\text{O.D. of non-heme protein}}{\text{O.D. of total protein}} \right) \text{poisoned} / \left(\frac{\text{O.D. of non-heme protein}}{\text{O.D. of total protein}} \right) \text{control}$$

where O.D. represents the optical density at 280 m μ .

When the ratio of non-heme protein to total protein in a control rat was 13%, it was defined as 100%.

RESULTS

Effects of toluene on rats:

Rats received daily injections of 2 ml. of a mixed solution of toluene and sesame oil in equal volumes per Kg. of body weight for three weeks.

The catalase activity in blood: The catalase activities in blood of rats received toluene for one week were in the range of 70—120%, whereas those of control animals were constantly 100% as reported in the previous paper⁷⁾ (Fig. 1). The

mean value of catalase activity at the seventh day was calculated to be 97%. This value is nearly the same with that of control. At the second week after the beginning of toluene injection, a sharp decline of about 20% was observed, but recovered to the normal level at the 3rd week.

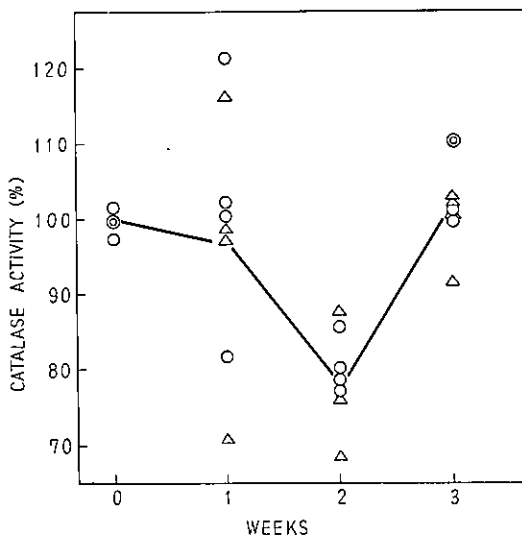


Fig. 1 Effect of toluene on the catalase activity in blood of rats.

○.....Rats received 2 ml. of a mixed solution of toluene and sesame oil in equal volumes.

△.....Rats received 4 ml. of a mixed solution of toluene and sesame oil in equal volumes.

When an enzyme solution decomposed 1.3×10^{-4} M of H_2O_2 per second, this enzyme solution was defined as having the activity of 100%. The assay of catalase activity was carried out at pH 6.8 and 0° .

From these experiments, it was elucidated that the values of catalase activity in blood of rats injected with toluene decreased similarly to those of rats injected with benzene⁷⁾, but it is really regrettable that the cause of recovery observed at the 3rd week remained still obscure.

In the above experiments, catalase activity was assayed at the final state by pretreating the enzyme with a small amount of H_2O_2 ⁷⁾.

Fig. 2 shows the relationship between $\log [H_2O_2]$ and the reaction time, in which $\log [H_2O_2]-t$ curve obtained from a poisoned rat bended with time (curve 2). When the enzyme solution was pretreated with a small amount of H_2O_2 , the curve became linear showing a constant inclination (curve 1) which ran parallel with the later part of curve 2. Therefore, if catalase activity is assayed at the initial state without pretreatment of H_2O_2 , the decrease of blood catalase activity will not be observed.

TOLUENE PISONING

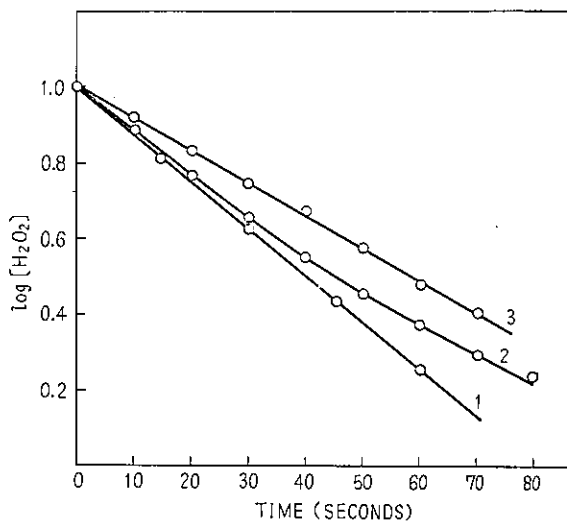


Fig. 2 Effect of pretreatment of H_2O_2 on the catalase activity in blood of rats injected with toluene.

The final concentration of H_2O_2 of pretreatment was 1/2000M, and the catalase reaction was initiated by adding much amounts of H_2O_2 (1/100M in final concentration). The assay of catalase activity was performed at pH 6.8 and 0° .

Curve 1: the reaction curve for a normal rat obtained with and without pretreatment of H_2O_2 .

Curve 2: the reaction curve for a rat injected with toluene for two weeks obtained without pretreatment of H_2O_2 .

Curve 3: the reaction curve for the same rat injected with toluene for two weeks obtained with pretreatment of H_2O_2 .

The bending of the reaction curve (curve 2) shows that the decrease of catalase activity in blood of rats injected with toluene is caused by a certain poisonous substance which inhibits reversibly the catalase reaction^{9,10}.

Fig. 3 shows the changes of the ratio of non-heme protein to total protein in erythrocytes endosoma. The values of the ratio decreased in about 50% at the seventh day after the beginning of toluene injection, and recovered to the normal level at the 3rd week.

The effect of toluene upon the recovery from benzene poisoning:

In the study of toluene poisoning, it was found that both the catalase activity in the blood and the ratio of non-heme protein to total protein in erythrocytes endosoma decreased in rats injected with toluene, which were also observed in rats injected with benzene as reported previously⁷. Basing upon these findings, the effect of toluene on the recovery from benzene poisoning was investigated.

Two ml. of a mixed solution containing the same amount of benzene and sesame oil per Kg. of body weight was injected subcutaneously into rats daily for three weeks. From the 22nd day, one group of benzene poisoned rats received daily

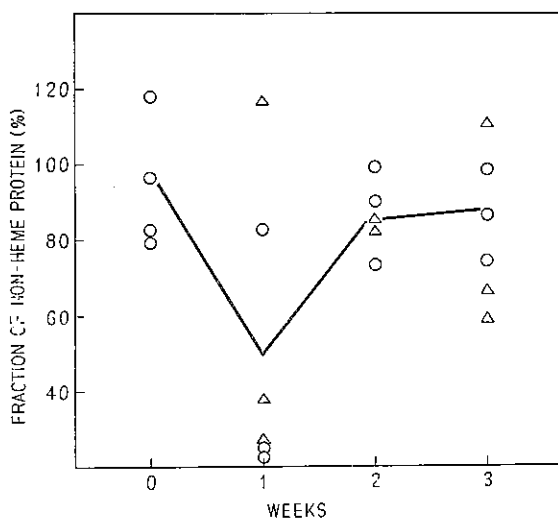


Fig. 3 The ratio of non-heme protein fraction in erythrocytes endosoma of poisoned rats against that of control animals.

○.....Rats received 2 ml. of a mixed solution of toluene and sesame oil daily.
 △.....Rats received 4 ml. of a mixed solution of toluene and sesame oil daily.

Ordinate: the percentage of the ratio, (non-heme protein/total protein) of poisoned rat/ (non-heme protein/total protein) of control rat. When the ratio of non-heme protein to total protein in a normal rat was 13%, it was defined as 100%.

injections of 2 ml. of a mixed solution of toluene and sesame oil in equal volumes instead of benzene for two weeks, and the other one group of benzene poisoned rats received injections of sesame oil only for two weeks.

Fig. 4 shows the effect of toluene which was decreased with benzene injection. Following daily injection of benzene, the first fall of activity was observed at the seventh day and the mean value was calculated to be 80%. Then, it recovered to the normal level at the 2nd week, but at the 3rd week a severe decline was again observed. Those changes have been already reported by us⁷⁾. By discontinuing the injection of benzene, the decreased catalase activity (70–80%) recovered rapidly to the normal level, 100%, while the catalase activity of rats injected with toluene instead of benzene did not show such remarkable change as shown in the figure.

As shown in Fig. 5, the ratio of non-heme protein to total protein in erythrocytes endosoma of benzene treated rats showed a sharp decline in three weeks after the beginning of injection. The decreased ratio recovered to the normal level as soon as discontinuing the injection of benzene, which was observed in both groups of animals injected with toluene and oil only.

The number of leucocytes which decreased markedly with benzene injection recovered to the initial value as soon as discontinuing the injection of benzene as shown in Fig. 6, in which the effect of toluene was not observed.

TOLUENE PISONING

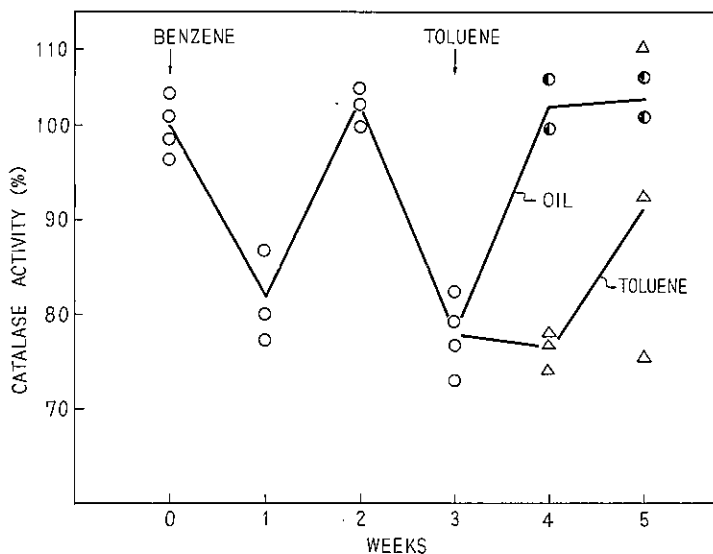


Fig. 4 Effect of toluene on the recovery of catalase activity in blood of rats injected with benzene.

Rats received 2 ml. of a mixed solution of benzene and sesame oil in equal volumes for three weeks. One group of rats injected with benzene received 2 ml. of a mixed solution of toluene and sesame oil in equal volumes for two weeks and the other one group of rats treated with benzene received oil only for two weeks.

The assay of catalase activity was made at pH 6.8 and 0°.

DISCUSSION

In the previous paper⁷, it was reported that the catalase activity in blood of rats injected with benzene dropped to 30% of that of control animals, which suggests that the assay of the catalase activity is contributable to the diagnose of benzene poisoning in its early stage.

In the experimental toluene poisoning, the decrease of the catalase activity in blood was also observed as shown in Fig. 1, which was caused by an unknown poisonous substance accumulated in blood and not by the decrease of the total amounts of catalase in blood. The interaction between the catalase molecule and this unknown poisonous substance seemed to be reversible as reported previously in the study of benzene poisoning⁷, namely;



where E represents the catalase molecule, G an unknown poisonous substance, and EG an inactive complex.

Urata⁸ reported that the catalase activity which was assayed by using an excessively diluted enzyme solution according to the method reported by Euler and

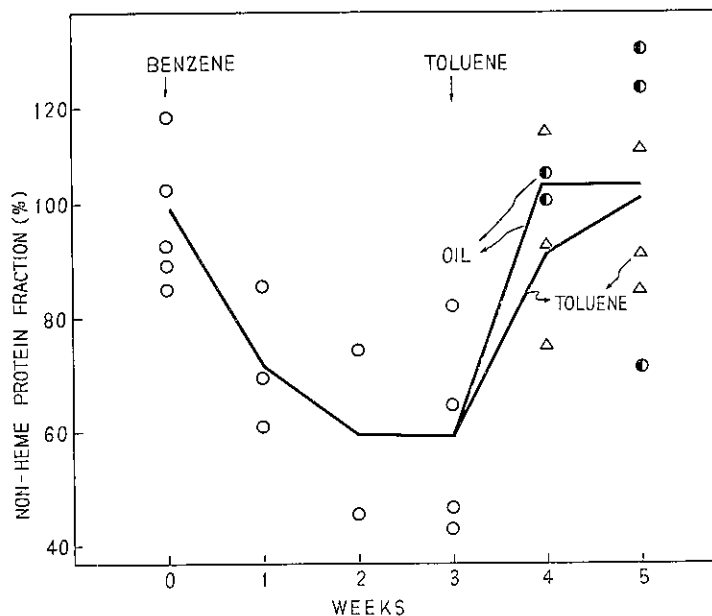


Fig. 5 Effect of toluene on the recovery of the ratio of non-heme protein to total protein in erythrocytes endosoma of rats injected with benzene.

Rats received 2ml. of a mixed solution of benzene and sesame oil in equal volumes per Kg. of body weight for three weeks. One group of rats injected with benzene received 2ml. of a mixed solution of toluene and sesame oil in equal volumes per Kg. of body weight for two weeks and the other one group of rats treated with benzene received oil only.

Ordinate: the percentage of the ratio, (non-heme protein/total protein) of poisoned rats/(non-heme protein/total protein) of control. When the ratio of non-heme protein to total protein in a normal rat was 13%, it was defined as 100%.

Josephson¹¹⁾ was not decreased by toluene administration. This result does not coincide with the result obtained by us. This discrepancy may be explained as follows: His result was obtained by determining the activity of an excessively diluted enzyme whereas our experiments were carried out much higher concentrations of enzyme at the final state. If catalase activity is assayed by using an excessively diluted enzyme solution which is prepared by diluting the blood of a toluene poisoned rat with large amounts of water, the decrease of catalase activity will not be probably observed, because the reaction (A) will proceed to the left and most of the catalase molecule will be present in active state.

El Masri et al¹²⁾ reported that toluene converted to benzoic acid in the body and was excreted in the form of hippuric acid. It was ascertained by us that these metabolites are not the unknown poisonous substance for catalase action, because 10^{-2} M of benzoic acid and of hippuric acid do not inhibit the catalase action at pH 6.8 and 0°.

TOLUENE PISONING

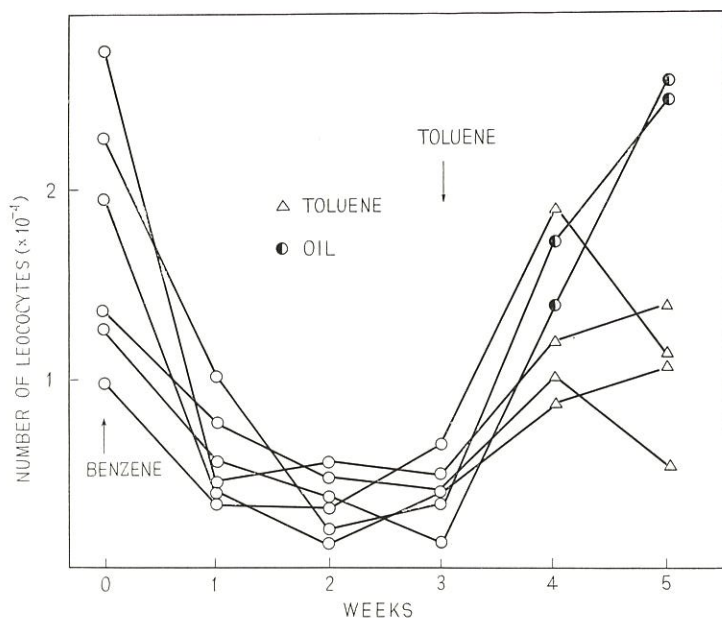


Fig. 6 Effect of toluene on the recovery of the number of leucocytes in rats injected with benzene.

Rats received 2ml. of a mixed solution of benzene and sesame oil in equal volumes per Kg. of body weight for three weeks. One group of rats injected with benzene received 2ml. of a mixed solution of toluene and sesame oil in equal volumes per Kg. of body weight for two weeks and the other group of rats treated with benzene received oil only.

The decreased catalase activity in blood of rats injected with benzene recovered to the normal level as soon as discontinuing the injection, while the activity was kept in the same level in the animals injected with toluene daily after the cessation of benzene treatment. These facts may indicate that the unknown poisonous substance accumulated in blood by injecting with benzene is excreted very rapidly, and that toluene suppresses the process of the excretion or that a new poisonous substance produced following toluene administration is accumulated in blood. At any rate, it is clear that toluene has a severe effect on the recovery process from benzene poisoning.

This finding was also ascertained in man. Fig. 6 shows the catalase activities in blood of workers in a paint-spraying plant using toluene as a main solvent. In this plant, benzene had been used as a main solvent before toluene was. A significant difference was observed between A-group employed after toluene was used as a main solvent and B-group employed before. This fact also shows distinctly that toluene has a significant effect on the recovery from benzene poisoning.

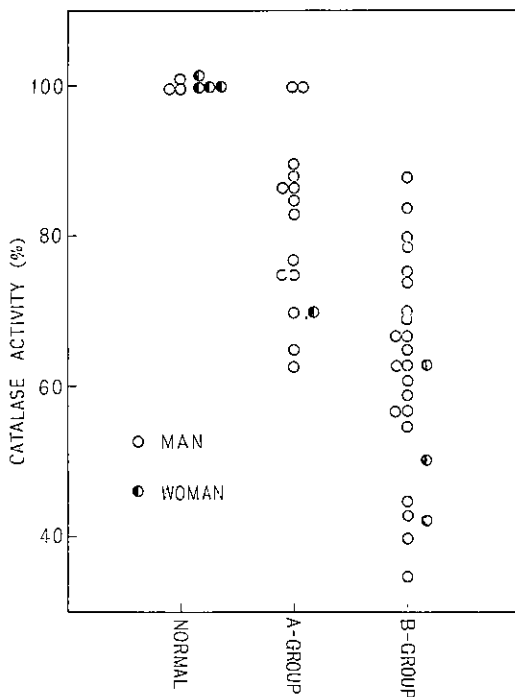


Fig. 7 Catalase activity in blood of workers who were working at a paint-spraying plant using toluene as main solvent.

A-group: men who were employed after toluene was used as main solvent instead of benzene.

B-group: men who were employed before toluene was used.

The assay of catalase activity was performed at pH 6.8 and 0°.

SUMMARY

1. The catalase activity in blood and the ratio of non-heme protein to total protein in erythrocytes endosoma decreased by injecting with toluene.

2. It was ascertained that the decrease of the catalase activity in blood was caused by an unknown poisonous substance accumulated in blood.

3. Following the administration of toluene, no remarkable effect was noticed on the recovery process of the ratio of non-heme protein to total protein in erythrocytes endosoma of rats pretreated with benzene. While a striking effect of toluene was observed on the recovery process of catalase activity in rats which were injected with benzene previously.

REFERENCES

- 1) Browning, E., : Toxicity of Industrial Organic Solvents, Her Majesty's Stationary Office, 3, (1953).

TOLUENE PISONING

- 2) El Masri, A.M., Smith, J.N. & Williams, R.T., : Biochem. J., 64, 50, (1956)
- 3) Svirbely, J.L., Dunn, R.C. & von Oettingen, W.F., : J. Indust. Hyg., 25, 366, (1943).
- 4) Ishizu, S., : Jap. J. Indust. Health, 2, 291, (1960).
- 5) Hirasawa, I., : Jap. J. Public Health, 7, 631, (1960).
- 6) Urata, J., : Jap. J. Indust. Health, 3, 20, (1961).
- 7) Hasegawa, H. & Sato, M., : Bull. Nat. Inst Indust. Health, 2, 17, (1960).
- 8) Sato, M. & Hasegawa, H., : ibid, 3, 1, (1960).
- 9) Ogura, Y., Tonomura, Y., Hino, S. & Tamiya, H., : J. Biochem., 37, 153, (1950).
- 10) Ogura, Y., Tonomura, Y., Hino, S. & Tamiya, H., : ibid, 37, 179, (1950).
- 11) von Euler, H. & Josephson, K., : Acta. Chemica. Scand., 1, 42, (1947).

要 旨

トルエン中毒の実験的研究及びベンゼン中毒の回復過程に 及ぼすトルエンの影響について

長谷川 弘道 佐藤 光男

ベンゼン中毒の惨状が報告されるにつれて、ベンゼンに代わる溶剤としてトルエンが取上げられるに至った。然し、トルエンの毒性に関する研究の歴史は浅く、特にベンゼンからトルエンへの切替え時に際して、トルエンの生体に及ぼす影響については未だみるべき研究はない。

先に私共はベンゼン中毒時にラットの血液中のカタラーゼの活性が顕著に低下すること、又赤血球内漿の蛋白質の組成比に変化が起ること等を報告したが、同様な現象が、トルエン中毒（ラット）でもみられることを確めた。

カタラーゼ活性の低下はカタラーゼ分子に或る毒物が結合してカタラーゼを不活性化するためにおこることが判った。

El Masri 等はトルエンは生体内で安息香酸及び馬尿酸に代謝されることを報告しているので、之れ等の代謝物がカタラーゼ作用に対して阻害作用を示すかどうかを $10^{-3} M$ の高濃度のこれ等の溶液を使って調べたが、カタラーゼ反応は全く阻害されないことが判った。即ちこの未知の阻害物質は安息香酸又は馬尿酸以外のものである。

ベンゼン投与によってカタラーゼ活性の低下したラットについて、トルエン投与の影響をしらべたところ、トルエンを与えない群ではその活性はすみやかに正常値まで回復するが、トルエンを与えた群では活性の回復はみられず、明らかにトルエンが影響していることがわかった。トルエンの投与を開始して一週間以内にはカタラーゼ活性の低下は認められないから、上記の実験でトルエンは、ベンゼン投与によって生じたカタラーゼ反応阻害物質^{?)}の排泄を妨げるものと解釈出来るがその決定は今後の実験にまちたい。

THE TOXIC EFFECT OF THE VARIOUS DUSTS ON THE INTRAPERITONEAL MONOCYTE IN RAT

Kimiko KOSHI, Hisato HAYASHI, Akira HAMADA and Hiroyuki SAKABE

In the previous paper the authors¹⁾ studied on the change of quartz particles caused by grinding and their toxicity to intraperitoneal monocyte in rat. It was found from these observations that the toxicity of quartz dust to the cultured phagocytic cells decrease with increase of grinding time, and these decreased toxicity is recovered by alkali leaching. Physicochemical analysis showed that the surfaces of quartz dusts were changed into different structure by grinding. Some of the authors²⁾ studied on the fibrogenic activities of these ground and alkali leached quartz dusts by intraperitoneal injection method and found a correspondence between the cellular toxicity in vitro and fibrogenic potency in vivo. Recently, this parallelism was also reported by Marks et al³⁾, Pernis et al⁴⁾, and Saffiotti et al.⁵⁾

The present paper describes the toxic effect of various mineral dusts on the monocyte of rat.

EXPERIMENTAL MATERIAL AND METHOD

1). Culture Procedure and Determination of Cell Activity.

The cells were obtained from exsudate induced in male rat of Wister strain by intraperitoneal injection of 5 ml. of sterile Tyrode's solution containing 0.01% glycogen. That is, the exsudate obtained 2 days after injection was washed with sterile Tyrode's solution containing 12 units of heparin per ml., and then the cells were separated from this heparinized solution by centrifugal separation at 1,000 r.p.m. for 5 minutes and washed twice with sterile Tyrode's solution. The cells were suspended in the culture medium. As culture medium, the sterile Tyrode's solution containing 30% of rat serum was used.

As culuture chambers, the following two kinds of tube were used: a test tube with double rubber cap for determination of dehydrogenase activity and square tube with capacity of 10 ml. in which a small piece of cover glass was placed.

The cell cultures containing 4 million cells in one ml. of medium were incubated at 37°C for 24 hours without addition of dust.

For the determination of dehydrogenase activity, varying amounts of each dust which was suspended in one ml. of medium, were added to the cultures and the cultures were incubated at 37°C for three hours. After contacting has been made between cells and dusts, the indicator system of tetrazolium and cysteine in Tyrode's

TOXIC EFFECT OF VARIOUS DUSTS ON MONOCYTE

solution was added to the mixture according to the method by Marks⁹⁾. Then, the mixture was incubated in 37°C water bath for 1.5 hours and the reaction was stopped with acetone. The amounts of reduced tetrazolium were estimated by electro-photometrical spectrophotometer at 490 m μ . Details of the methods of collecting cells, sterilization, dispersion of dust, determination of dehydrogenase activity and of morphological examination were described in the previous papers,¹²⁾ but sterilization of the sample was not performed because the heat treatment may produce any change of crystal state of clay mineral by dehydration. The other hand, for morphological examination 200 μ g of each dust was added to cultured cells and after 3 hours cover glass on which cells adhered was taken out from culture tube. The cells on the cover glass were fixed with methanol and were stained with Giemsa solution.

2). Dust Sample

The minerals which were used in this study are shown in Table 1. The purity of these mineral samples was examined by x-ray analysis. The size of each dust sample was ascertained by electronmicrograph.

Table 1 Samples used in this work

No.	sample	composition	locality
1	Sphalerite	ZnS	Asahi mine, Niigata Prefecture
2	Pyrite	FeS ₂	Kishu mine, Wakayama Prefecture
3	Flourite	CaF ₂	unknown
4	Quartz	SiO ₂	Ishikawayama, Fukushima Prefecture
5	Tridymite	SiO ₂	Kusatsu, Gumma Prefecture
6	Cristobalite	SiO ₂	Utsunomiya Tochigi Prefecture
7	Fused silica		
8	Microcline	KAl Si ₃ O ₈	Ishikawayama, Fukushima Prefecture
9	Albite	(Na, Ca) Al (Al, Si) Si ₂ O ₈	Shikanoya, Gifu Prefecture
10	Diospide	CaMgSi ₂ O ₆	Unazuki, Toyama Prefecture
11	Asbestos	Mg ₃ Si ₂ O ₅ (OH) ₄	Nozawa mine, Hokkaido
12	Beryl	Be ₃ Al ₂ Si ₆ O ₁₈	Yamanoo, Ibaragi Prefecture
13	Olivine	(Mg, Fe, Mn) ₂ SiO ₄	Akaishi, Doitown, Ehime Prefecture
14	Topaz	Al ₂ (F, OH) ₂ SiO ₄	Obira mine, Ōita Prefecture
15	Cyanite	Al ₂ SiO ₅	India
16	Tourmaline	XY ₃ Al ₆ (OH) ₄ (BO ₃) ₃ Si ₆ O ₁₈ X=Na, Ca, rarely K, Y=Mg, Al, Li, Fe etc.	Obira mine, Ōita Prefecture
17	Muscovite	K ₂ (Al, Fe, Mg) ₄ (OH) ₄ (Si, Al) ₈ O ₂₀	Weke, Ishikawayama, Fukurhima, Prefecture
18	Sericite	same above	Yoji pass, Gumma Prefecture
19	Sericite	same above	Nasu mine, Tochigi Prefecture
20	Sericite	same above	Hitachi, Ibaragi Prefecture
21	Chlorite	(Mg, Fe, Al) ₆ (OH) ₈ (Si, Al) ₄ O ₁₀	Hanaoka mine, Akita Prefecture
22	Talc	Mg ₃ Si ₄ O ₁₀ (OH) ₂	Kanjon, Chaina
23	Pyrophyllite	Al ₂ Si ₄ O ₁₀ (OH) ₂	Honami mine, Nagano Prefecture
24	Halloysite	Al ₄ (OH) ₈ Si ₄ O ₁₀ nH ₂ O	unknown
25	Kibushi-clay		
26	Anthracite		Omine coal field
27	Diatomaceous earth		Hitoyoshi, Kumamoto Prefecture
28	Obsidian		Wada pass, Nagano Prefecture

X-ray powder refractions were recorded by x-ray diffractometer. Experimental conditions were as follows: Filtered Cu radiation, 30 Kv., 15 mA. slit system, 2 mm., 1.5 mm., 1 mm., scanning speed 1° per minute.

For quantitative analysis, the method of Sudo, Oinuma and Kobayashi⁽⁹⁾⁽¹⁰⁾ was used. Specimen powder was kneaded with a small amount of water on the glass slide. And then water was added drop by drop. Uniformity of the specimen film was examined by transmitted light. Finally, the slide was dried in room air.

The specimen powder was spread over on glass slide in fixed area of 2.0 x 2.7 cm in well-orientated aggregates. Peak intensities increased with increasing amount of powder. But, if the amounts of specimen increased over some level, they gradually decreased, because the parallel orientation is disturbed by increase of the amount of a specimen per unit volume. We preferred to 0.04 gram as the amount to be taken for a film with a fixed area of 2.0 x 2.7 cm.

RESULTS AND DISCUSSION

1) Effect of Particle Size of Dust on the Dehydrogenase Activity of the Cultured Monocytes.

Marks et al⁽⁹⁾. reported that toxic effect of very fine silica dust (0.5 microns or less) on the dehydrogenase activity in the cells could not be examined satisfactorily in quantitative manner because these particles tended to adhere to one another and the degree of particle dispersion varied with different experiments. Therefore, we examined the effect of particle size on the dehydrogenase activity of intraperitoneal monocytes in advance of the estimation of toxic dosis of various mineral dusts. For the experiment, two series of quartz particles of various sizes were used. One series was original quartz particles. Quartz was ground by hand in agate mortar for 2 minutes, and then the particles of 0.5 or less, 0.5 to 1.5, 1.5 to 3.0, 3.0 to 5.0, 5.0 to 10.0 and 10.0 to 15.0 microns were collected separately by water elutriation. The other series was leached quartz. Original quartz particles were leached with 10% NaOH solution, and the particles were sized by the same method as above. The electron micrographs and micrographs of these samples are shown in Fig. 1.

Two hundreds μg of each sample was added to cultured tubes and then the cultures were incubated for 3 hours. After incubation, tetrazolium reducing capacity of the culture was compared with that of control ones. The results are shown in Fig. 2.

As seen in the figure, toxicity of original quartz was not directly related to the particle size. That is, the highest toxicity was observed at the size of 1.5 to 3.0 microns and toxicity of smaller or larger particles than this size decreased with the decrease or increase of particle size. However, the toxicity of leached quartz was directly related to the particle size. From these results, it was assumed that the surfaces of finer dusts might be more modified by grinding than the coarser

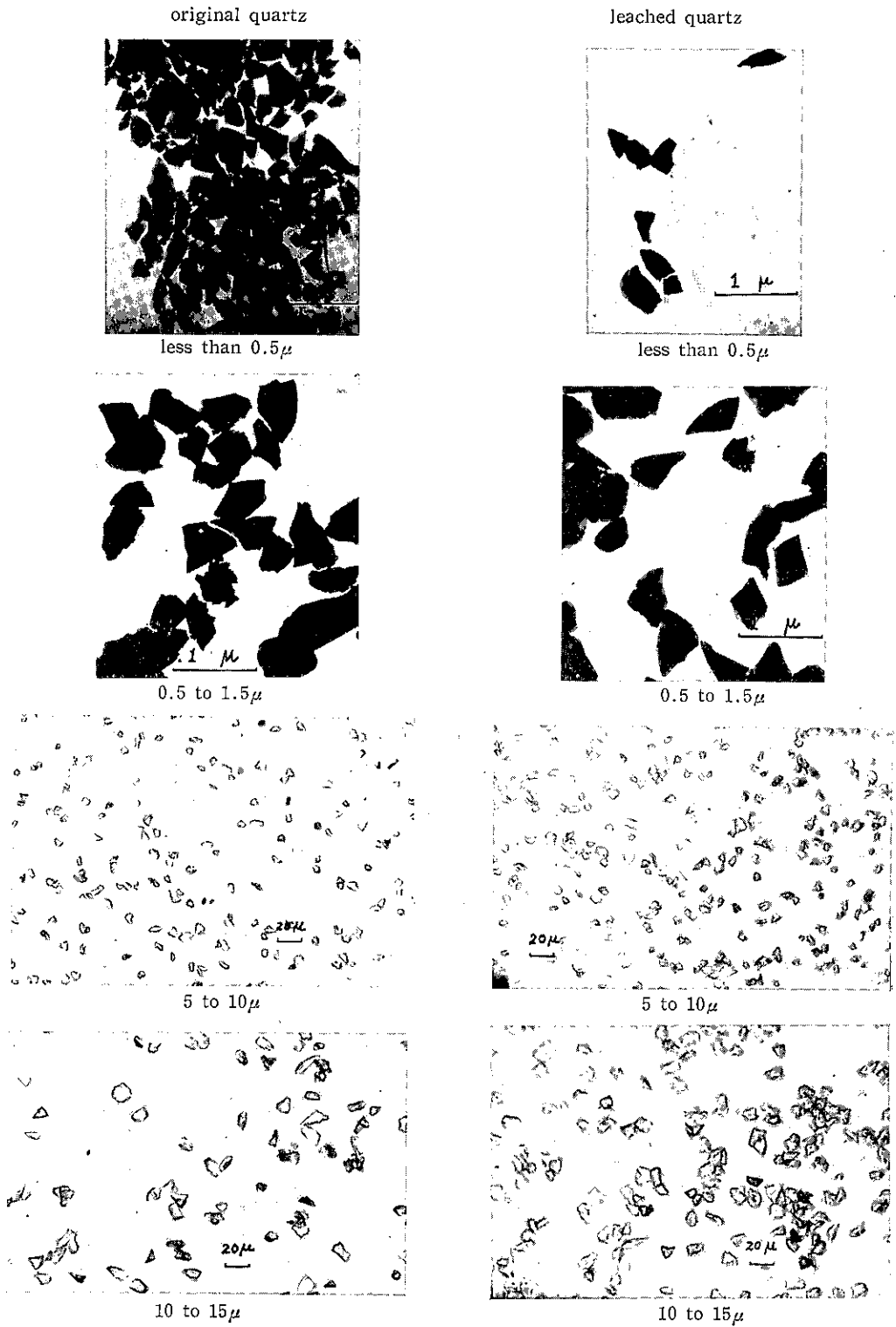


Fig. 1 Electronmicrographs and micrographs of original and leached quartz of various sizes.

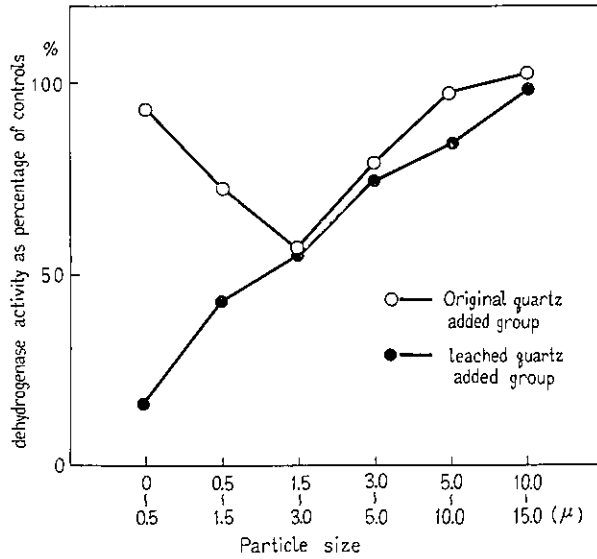


Fig. 2 The relation between the toxicity and particle size of quartz. 200 μ g of original and leached quartz were added to cultured monocyte and then the cultures were incubated for 3 hours. After incubation, tetrazolium reducing capacity of these cultuers was compared with that of control ones.

ones.

Then the toxicity of sericite samples (Yoji) of 1 or less, 1 to 2, 2 to 5, 5 to 10 and 10 to 25 microns sizes was estimated. The micrograph of sericite sample is shown in Fig. 3. The determination of dehydrogenase activity in cultures was carried out as described above. The results are shown in Fig. 4. As seen in Fig. 4, the effect of particle size of sericite on the dehydrogenase activity showed a similar tendency to the result obtained by the original quartz particles. The monocytes which phagocytosed

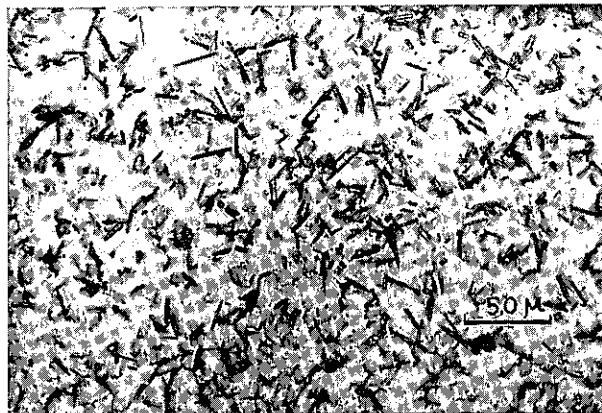


Fig. 3 Micrograph of sericite particles of 10 to 25 μ size (Yoji).

TOXIC EFFECT OF VARIOUS DUSTS ON MONOCYTE

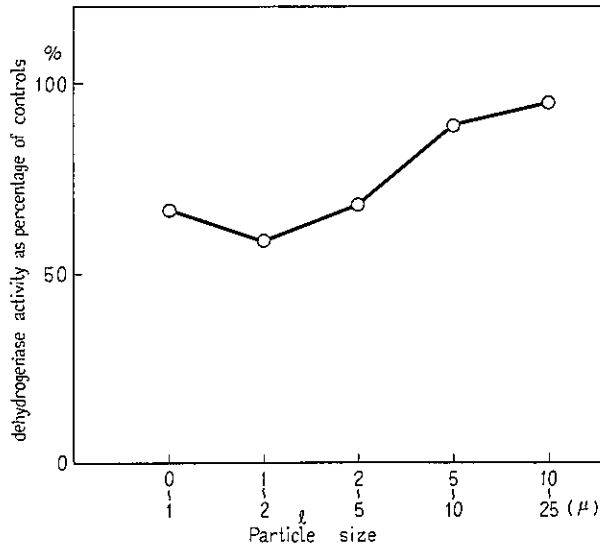


Fig. 4 The relation between the toxicity and particle size of sericite (Yoji).

200 μ g of sericite (Yoji) of each size was added to cultured monocyte and then the cultures were incubated for 3 hours. After incubation, tetrazolium reducing capacity of these cultures was compared with that of control ones.

sericite particles are shown in Fig. 5. As seen in micrographs of phagocytic monocytes, no adhesion was found in these dusts and damage was obvious in the cells which phagocytosed the sericite of 1 to 2 microns, while no damaged cells were found among the cells which phagocytosed the sericite of 10 to 25 microns. From these results, dust particles of 0.5 to 2 microns in diameter were used in next experiment for the determination of toxic doses of various mineral dusts to monocytes.

2) Toxic Doses of Various Mineral Dusts to Intraperitoneal Monocyte.

The localities and results of X-ray analysis of minerals which were used in this study are shown in Table 1, Fig. 6 and supplement table.

Particles of 0.5 to 2 microns in diameter were separated by sedimentation and centrifugal separation in distilled water from small particles obtained by crushing, taking into account of the size effect shown in the preceding experiment. But, the asbestos particles were prepared under the size of 5 microns, as the small particles could not be obtained by crushing in asbestos.

The toxic doses of these dusts were estimated by tetrazolium reducing capacity of cultured monocytes. The toxic dose was expressed as the amount of dust necessary to depress by 50% the dehydrogenase activity of standard cultures of phagocytic cells. These results are summarized in Table 2. As for silica dusts, toxic doses were under 100 μ g., while those of sericite (Hitachi) was from 100 to 200 μ g, and of opal, pyrophyllite, talc, sericite (Yoji) and kibushi-clay, were from 200 to

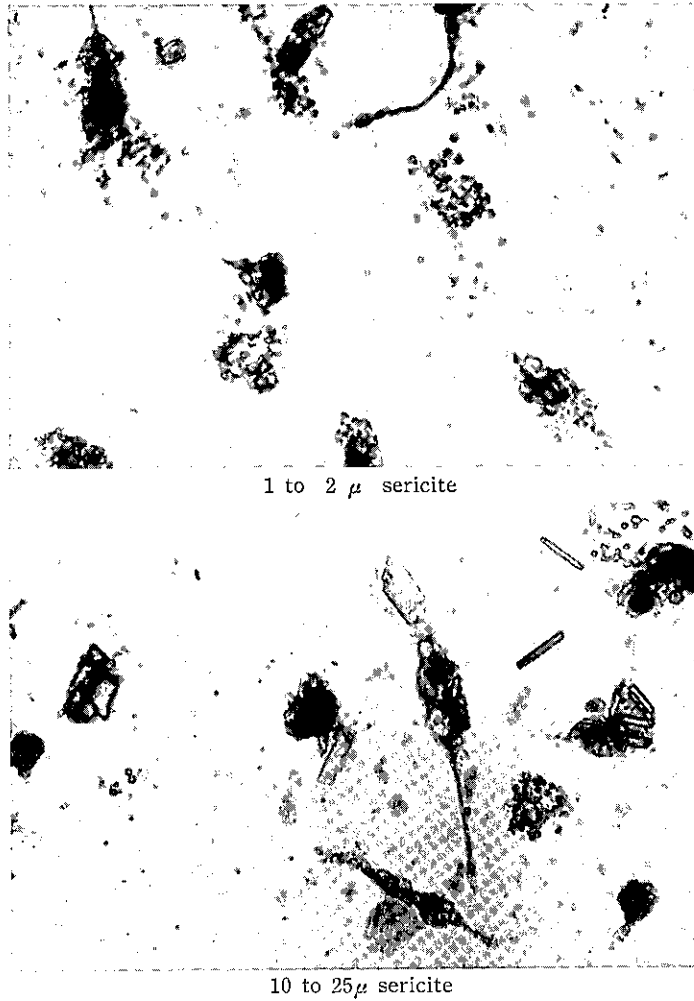


Fig. 5 The micrographs of the cultured monocytes phagocytosed with sericite (Yoji) (Giemsa-staining).

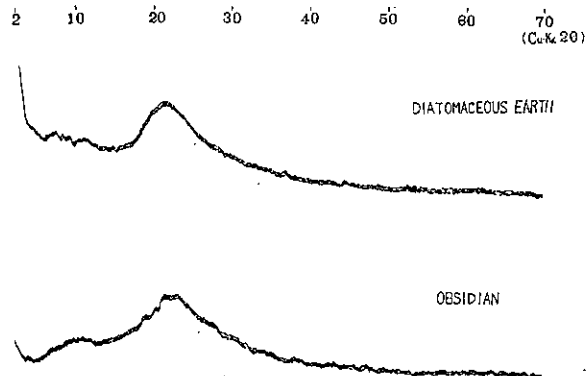


Fig. 6 The X-ray diffraction patterns of diatomaceous earth and obsidian.

TOXIC EFFECT OF VARIOUS DUSTS ON MONOCYTE

Table 2, The toxic doses of various mineral dusts (The particle size of 0.5 to 2 microns)

under 50 μ g	50 to 100 μ g	100 to 200 μ g	200 to 400 μ g	400 to 700 μ g	700 to 1,000 μ g	above 1,000 μ g
tridymite	NaOH leached quartz quartz (ground for 2 minute) fused silica cristobalite	sericite (Hitachi)	opal pyrophyllite talc sericite(Yoji) Kibushi-clay	topaz fluorite tourmaline cyanite diatomaceous earth sericite (Nasu) halloysite sphalerite	olivine asbestos*	microcline chlorite diopside obsidian albite beryl pyrite NaOH leached obsidian muscovite anthracite

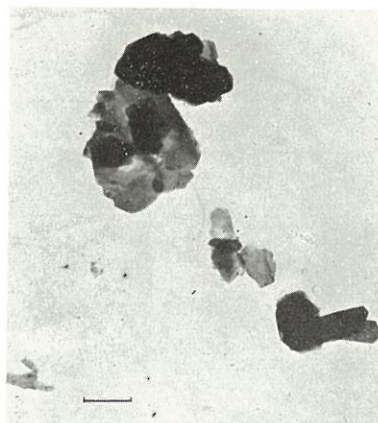
* The particle size of asbestos was less than 5 microns

400 μ g. The toxic doses of the other silicates were above 400 μ g. Rather high toxicity of sericite (Hitachi) seems to be produced by the contaminated alpha-quartz (about 10%). The difference of toxic doses between Yoji and Nasu sericite may be due to the difference of shape, as the latter consists of only flaky crystal, while in the former there are needle shaped crystal besides flaky one. Electronmicrographs of these two sericite are shown in Fig. 7.

The toxic dose of Kibushi-clay was relatively high, but this clay contained about 10% quartz, therefore it may be assumed that the toxic substance was not kaolin mineral but quartz. By the analytical method using x-ray diffraction the quartz less than 5



Yoji sericite



Nasu sericite

Fig. 7 The electronmicrographs of the sericite of Yoji and Nasu. Nasu sericite consists of only flat crystals with distinct hexagonal outline, but Yoji-sericite had needle-shaped particles besides flaky crystals.

The linear dimension on the micrographs represents 1 micron.

mg, could not be detected, but the tetrazolium reducing capacity of the intraperitoneal monocyte was influenced by quartz particles of the order μg . Therefore, it could not be concluded that the toxic actions of some silicates which showed relatively high toxicity are due to silicates only. However, it was very interesting that pure pyrophyllite, talc and sericite in which no impurity was found by x-ray diffraction, were relatively toxic. From these results, it was assumed that there is a considerable correlation between the cell toxicity of dust and lung fibrosis which was produced by dust in experimental animals or pneumoconiosis of workers. However, it must be noticed that the fine particles of asbestos showed rather low toxicity.

3), Toxic Doses of some Dusts collected in Plants.

The toxic doses of two sorts of dusts produced by arc welding and two sorts of silica fumes from electric furnace in silicon producing plants were estimated. Dusts

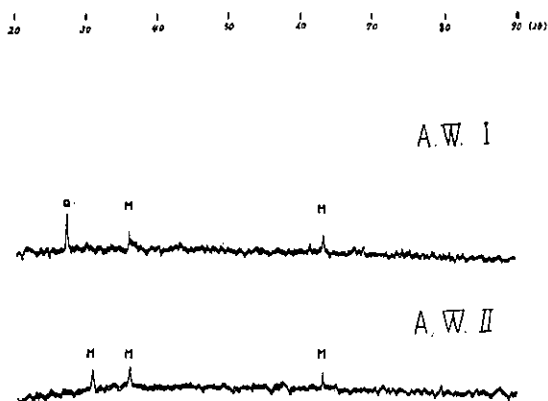


Fig. 8 X-ray diffraction pattern of arc welding dust 1 and 2.
Q.....quartz, M.....magnetite



Fig. 9 Electronmicrograph of silica fume 1 in plant.

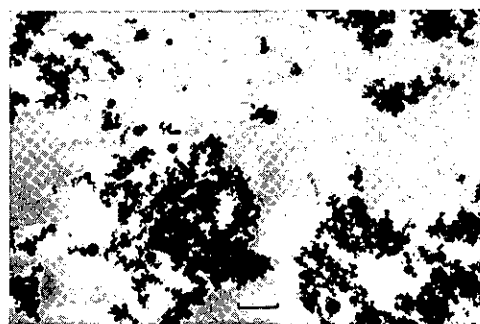


Fig. 10 Electronmicrograph of silica fume 2 in plant.

The linear dimension on the micrograph represents 1 micron.

TOXIC EFFECT OF VARIOUS DUSTS ON MONOCYTE

under 2 microns collected by water elutriation were used. The x-ray diffraction patterns of two sorts of arc welding dusts are shown in Figure 8. As seen in Figure 8, from x-ray analysis, arc welding dust-1 contained free silica but arc welding dust-2 did not. The toxic dose of the former was 380 μg , and of the latter was 1,000 μg . The electronmicrographs and the x-ray diffraction patterns of two sorts of silica fumes are shown in Figure 9, 10 and 11. The silica fume-1 was estimated to contain 14.4% of free silica according to phosphoric acid method (by Schmidt)¹⁰ and silica fume-2 had no silica. The toxic dose of silica fume-1 was 360 μg , and that of silica fume-2 was above 1,000 μg . From these results, it may be assumed that toxic action to monocyte caused not only by silica fume and magnetite of arc welding dust but by quartz in these dusts.

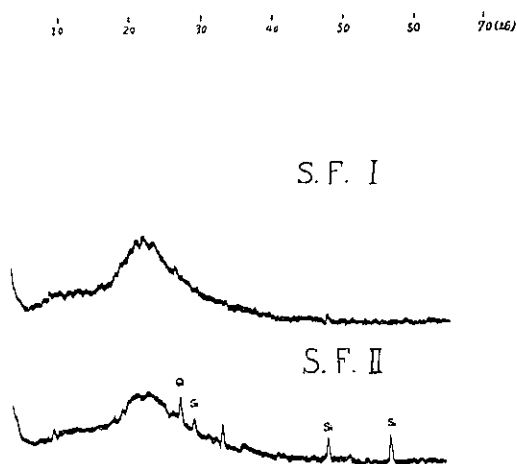


Fig. 11 The X-ray diffraction pattern of silica fume 1 and 2.
Q.....quartz, Si.....silicone

SUMMARY

1. Effect of particle size of dust on the dehydrogenase activity of the cultured monocytes was studied. Cell toxicity of dust, which was supposed from the inhibition of this enzyme activity, increased with the decrease of particle size in leached quartz, but it did not correlate in such a manner to the particle size under about 2 microns in original quartz or sericite.

2. Toxic doses of the following mineral dusts to the monocytes were estimated using tetrazolium reducing capacity, and it was found that the toxicity of dust decreased in the order of following group: group 1. - tridymite, group 2. - NaOH leached quartz, quartz ground by hand for 2 minutes, fused silica, and cristobalite, group 3. - sericite (Hitachi), group 4. - opal, pyrophyllite, talc, sericite (Yoji), and

K. KOSHI, H. HAYASHI, A. HAMADA AND H. SAKABE

Kibushi-clay, group 5. - topaz, fluorite, tourmaline, cyanite, diatomaceous earth, sericite (Nasu), halloysite, and sphalerite, group 6. - olivine and asbestos, group 7. - microcline, chlorite, diopside, obsidian, albite beryl, pyrite, muscovite and anthracite.

3. Cell toxicity of arc welding and silica fumes collected in plants was also investigated, and discussed on the role of contaminated free silica.

ACKNOWLEDGEMENT

We wish to express our thanks to Prof. T. Sudo of Tokyo University of Education for his kind suggestion and to Miss M. Yasukawa in our Institute for her technical assistance. The authors are also indebted to Prof. H. Shibata, Dr. H. Kodama, Mr. M. Sato and Mr. K. Harada of Tokyo University of Education, to Dr. H. Takahashi and Dr. H. Minato of Tokyo University, and Dr. N. Fusamura, Dr. R. Otsuka and Mr. A. Ishii of Waseda University for presentation of samples.

REFERENCES

- 1) Sakabe, H., Kawai, K., Koshi, K., Soda, R., Hamada, A., Shimazu, M. and Hayashi, H.: Bull. Nat. Inst. Indust. Health, 4, 1, (1960).
- 2) Sakabe, H., Kajita, A. and Koshi, K.: in this Bulletin.
- 3) Marks, J. and Nagelschmidt, G.: A.M.A. Arch. Indust. Health, 20, 383, (1959).
- 4) Pernis, B. and Vigliani, L.: Med. Lavoro, 51, 3, (1960).
- 5) Saffiotti, U., Tommasini Degna, A. and Mayer, L.: Med. Lavoro, 51, 518, (1960).
- 6) Marks, J. & James, D.M.: J. Path. and Bact., 77, 401, (1959).
- 7) Koshi, K., Kawai, K. and Sakabe, H.: Bull. Nat. Inst. Indust. Health, 2, 29, (1959).
- 8) Sudo, T., Oinuma, K. and Kobayashi, K.: Second Conference on clay mineralogy and petrography, Prague, May 10 th-17 th, (1961).
- 9) Schmidt, K.G.: Ber. D.K.G., 31, 402, (1954).
- 10) Oinuma, K. & Kobayashi, K.: Clay science, 1, 8, (1961). (printed in Japanese).

要 旨

種々鉱物性粉塵のラット腹腔内単核細胞に対する影響について

興 貴美子 林 久人 浜田 晃 坂部 弘之

著者らは、前報においてラット腹腔内単核細胞に対する石英粉末の影響を検討し、石英は磨砕する事によって、表面の構造が変化する事、及びこの表面の変化に伴って単核細胞に対する毒性の減弱する事を報告した。

そこで著者らは、更に石英以外の出来るだけ純粹にした種々の鉱物性粉塵について単核細胞に対する毒性を検討した。

供試鉱物性粉塵は第1表に示すように、石英の他、天然産トリヂマイト、溶融石英、方けい石、

TOXIC EFFECT OF VARIOUS DUSTS ON MONOCYTE

蛋白石、ろう石、タルク、木節カオリン、絹雲母(日立)、絹雲母(余地)、絹雲母(那須)、黄玉、ほたる石、黒曜石、珪藻土、無煙炭、緑泥石、白雲母、電気石、らん晶石、石綿、ハロイサイト、かんらん石、微斜長石、透輝石、曹長石、緑柱石、黄鉄鉱である。

これ等の鉱物の粉末を破碎して細粉化した後、水ひによって $0.5\sim 2\mu$ の粒度のものを集めた。(但し、石綿は破碎により細粉化する事が出来ないので 5μ 以下粒子とした。) これら粉塵の鉱物組成についてはX線回折により同定した。その結果は附表の通りである。

単核細胞に対する毒性の決定方法は、前報とほぼ同じである。即ち対照培養単核細胞のテトラゾリウム還元能 100 に対して、還元能を 50 に阻害するに必要な粉塵量である。但し、今回の実験では細胞と粉塵との接触時間は3時間とした。

各鉱物性粉塵の毒性量は、第2表に示した。

表によると、各種シリカ粉塵の毒性量は $100\mu\text{g}$ 以下であり、これによつて日立産絹雲母が高い毒性を示す。 $200\mu\text{g}\sim 400\mu\text{g}$ の毒性を示すものには、蛋白石、ろう石、タルク、絹雲母(余地)、木節カオリンがある。 $400\mu\text{g}\sim 1000\mu\text{g}$ の間の毒性量を示すものには、黄玉、ほたる石、電気石、けい藻土、絹雲母(那須)、石綿、ハロイサイト、かんらん石があり、その他の粉塵の毒性量は $1000\mu\text{g}$ 以上であった。このうち、日立産絹雲母及び木節カオリンはX線回折によつて約10%の α -石英を含んでいるので、毒性を示す物質が絹雲母及びカオリン鉱物であるのか混入している石英であるのかは判然としない。尚、今回用いたX線回折による定量法では石英に対する感度は 5mg 以上であるが、単核細胞に対する石英の毒性は μg order なので、他の鉱物に於いても、共存する石英の影響を全く無視する事は出来ないかも知れない。しかし、X線回折分析法において純粋と考えられる絹雲母(余地)、ろう石、タルクなどが比較的高い毒性を示す事は興味深い。

又、現場における電気熔接粉塵及びシリカフェームについて若干の実験を行った。これらの粉塵から 2μ 以下の粒子を選び、毒性量を求めると、X線回折及び遊り珪酸測定により石英を含む電気熔接粉塵並びにシリカフェームの毒性は、 $360\mu\text{g}$ 及び $380\mu\text{g}$ となるが、石英を含まぬ夫々の粉塵の毒性は $1,000\mu\text{g}$ 以上であった。

尚、上記粉末の毒性量の決定に先立って、粒子の大きさと毒性との間の関係を検討するため、手磨砕石英及び NaOH 処理石英について、 $0\sim 0.5$ 、 $0.5\sim 1.5$ 、 $1.5\sim 3$ 、 $3\sim 5$ 、 $5\sim 10$ 、 $10\sim 15\mu$ の各粒度のものの毒性を比較した。

結果は、第2図に示すようであつて、手磨砕石英では、 $1.5\sim 3\mu$ のものが最も毒性が強く、それより大きい粒子及び小さい粒子では毒性が弱くなる。しかし、NaOH 処理石英においては粒子が小さくなればなる程毒性が強い。この事は、前報の結果から考え、小さい粒子程、磨砕の影響を強く受けているためと考えられる。絹雲母(余地)における粒子の影響も手磨砕石英の結果と同じ傾向であつた。

SUPPLEMENT TABLE

Sphalerite			Melanterite			Pyrite			Flourite		
A		No.1	A		No.2	B		A		No.3	
d	I	d	I	d	I	d	I	d	I	d	I
3.95	3	3.48	<1	8.0	<1			3.149	7	3.14	162
		3.48	<1	6.8	<1			1.928	10	1.93	175
3.12	10	3.13	<1	6.0	<1			1.644	7	1.64	67
2.70	7	2.71	10	4.90	10	4.92	95	1.363	4	1.37	26
		2.13	25	4.55	1			References in this table A: C. T. De Assuncao et J. Garrido : Tables pour la détermination des minéraux au moyen des rayons x (1953) B: K. Kubo and S. Kato Chemical analysis by x-ray diffraction (1955) C: G. L. Kalousek and L. E. Muttart : Studies on the chrysotile and antigorite components of serpentine Am. Min. 42, 1-22 (1957) D: R. E. Grim : Clay mineralogy (1953) E: A.S.T.M. card			
1.91	9	1.92	1	4.02	1	3.75	12				
1.63	9	1.64	6	3.49	12	3.49	12				
1.555	3	1.57	17	3.53	15	3.53	15				
1.330	7	1.36	30			3.14	30				
1.241	8	1.245	60	3.23	2	2.71	87				
1.210	3	1.213	11	3.09	1	2.43	55				
				2.92	<1	2.22	47				
				2.75	1	2.01	16				
				2.63	2	1.92	42				
				2.50	<1	1.82	5				
				2.42	<1	1.63	72				
				2.31	1	1.57	17				
				2.17	<1	1.51	23				
				2.11	<1	1.453	20				
				2.07	<1	1.46	5				
				2.01	1						
				1.96	1						
				1.92	<1						
				1.87	1						
				1.81	<1						

Lattice Spacings (d) and Visually Estimated Relative Intensities (I) of X-ray Diffraction of Samples

TOXIC EFFECT OF VARIOUS DUSTS ON MONOCYTE

Quartz				Tridymite				Cristobalite				Microcline			
A		No.4		A		No.5		A		No.6		B		No.8	
d	l	d	I	d	I	d	I	d	I	d	I	d	I	d	I
4.24	4	4.29	204	4.8	5	4.75	12	5.0	1	4.29	63	6.47	mw	7.25	8
3.35	5	3.72	35	4.39	10	4.53	16	4.05	10	4.13	103	5.84	w-mw	6.51	11
2.45	3	2.47	88	4.12	10	4.29	212	3.15	4					5.94	7
2.285	3	2.287	83	3.73	9	4.06	212	2.85	5			4.16	ms	4.25	38
2.236	2	2.248	49			3.80	195	2.48	9	2.51	20			4.02	12
2.129	3	2.137	51	3.23	5	3.52	38					3.945	mw	3.99	14
1.981	3	1.985	46			3.24	46					3.80	m	3.83	29
1.811	4	1.821	132	2.94	5	3.15	28					3.67	mw	3.66	15vb
				2.77	2	3.15	28							3.49	39
1.667	3	1.678	41	2.94	5	2.95	74					3.44	ms	3.36	39vb
1.539	4	1.544	97	2.77	2	2.84	32					3.34	m-ms	3.28	79
1.447	2	1.455	21	2.49	7	2.54	11					3.28	s	3.25	102
1.412	1			2.49	7	2.48	80					3.21	vs	3.12	19vb
						2.37	20					3.16	mw	2.98	24
		1.386	73			2.30	42					3.02	m	2.90	26
		1.380	45	2.28	2	2.13	10					2.93	ms	2.77	10
1.376	4	1.377	76	2.11	2	2.08	14					2.87	ms	2.61	15
		1.373	74	2.07	2	1.97	14					2.75	m	2.61	15
		1.372	26	1.97	5	1.899	13					2.61	m	2.56	15
				1.88	2	1.866	13					2.56	mw-m	2.43	7
				1.77	2	1.780	7					2.51	m	2.43	7
				1.69	7	1.689	18					2.410	m	2.34	5
				1.62	5	1.618	12							2.17	19
				1.591	5	1.547	18							1.981	6
				1.528	7	1.530	23							1.929	6
				1.432	5	1.428	11							1.870	6
				1.371	2	1.396	16							1.807	27
														1.580	4vb
														1.517	7
														1.457	9
														1.431	6

K. KOSHI, H. HAYASHI, A. HAMADA AND H. SAKABE

Albite				Diopside				Asbestos				Beryl			
A		No. 9		B		No. 10		C		No. 11		A		No. 12	
d	I	d	I	d	I	d	I	d	I	d	I	d	I	d	I
6.41	6	6.42	11			15.5	41	7.37	100	7.38	215	9.4	4	8.12	220
5.90	2	5.91	6			9.31	12	6.6	vw			8.1	10		
5.33	2					8.59	20	5.75	vw			5.2	4	4.65	94
		4.23	7	4.44	5	4.27	10	4.53	15			4.7	6		
4.11	5	4.05	25	3.33	5	3.38	20	4.47	15	4.44	48	4.45	2	4.02	70
3.81	1	3.88	13	3.30	21	3.30	21	4.44	15	3.66	222	4.07	6	3.63	16
		3.76	27	3.23	80	3.25	31	3.66	100	3.04	30	3.67	5	3.37	38
3.70	2	3.69	30			3.14	28	2.93	vw	2.62	10	3.33	8	3.27	157
		3.51	11	2.98	100	3.00	54					3.23	2		
3.40	<1	3.38	14	2.94	70	2.96	37	2.45	w	2.46	25	3.07	6	3.05	52
3.21	10	3.21	100	2.89	10	2.91	27	1.84	w	1.834	10	2.92	8	2.88	164
		3.00	15	2.82	5			1.54	m	1.540	34	2.34	5	2.54	34
2.95	5	2.95	22					1.46	vw	1.465	6	2.34	4	2.33	13
2.86	1	2.88	9	2.56	10	2.72	15	1.22	vw			2.23	4	2.23	10
		2.77	5			2.57	23					2.16	4	2.17	14
2.64	1	2.64	6	2.53	40	2.53	43					2.09	2	2.00	20
2.55	3	2.56	10	2.29	10	2.32	14					2.02	6		
2.45	3	2.47	6	2.18	5	2.21	8					1.99	2		
2.40	1	2.42	5	2.146	20	2.16	15					1.86	3		
2.31	3	2.32	5			2.146	15								
2.18	<1	2.20	3	2.124	20	2.124	20					1.81	5	1.804	12
2.12	3	2.14	7	2.101	30	2.101	30					1.76	6	1.749	30
		2.10	4	2.034	10	2.034	10					1.72	4	1.722	12
2.01	3	1.993	3	2.002	5	2.002	5					1.64	6	1.637	14
1.974	2			1.959	5	1.977	5					1.61	5	1.603	8
		1.937	2												
1.887	4	1.895	3	1.830	5	1.830	5					1.583	5	1.578	9
1.846	2	1.855	3	1.809	5	1.809	5					1.551	4	1.540	7
1.821	4	1.834	7	1.748	40	1.758	10					1.526	6	1.521	16
1.799	<1	1.807	8	1.680	5							1.472	5	1.461	11
1.777	3	1.787	9	1.668	5							1.443	6	1.439	13
1.745	2											1.414	2		
1.714	3			1.622	20	1.631	15					1.381	5	1.373	8
1.663	2	1.600	2	1.612	20										
		1.975	3	1.560	5										
1.581	1			1.548	5										
1.528	2			1.520	10										
1.500	3					1.535	10								
1.457	4	1.465	5			1.508	10								
		1.435	4			1.429	10								
1.385	1														
1.374	1														

TOXIC EFFECT OF VARIOUS DUSTS ON MONOCYTE

Olivine				topaz				Cyanite				Tourmaline			
A		No. 13		B		No. 14		A		No. 15		A		No. 16	
d	I	d	I	d	I	d	I	d	I	d	I	d	I	d	I
5.12	2	7.44	125	4.21	w	7.2	17	4.49	1	4.48	19	6.5	8	6.46	50
3.90	6	5.13	44	3.692	s	4.46	9	4.33	1	4.35	23	5.7	2	5.07	18
3.73	2	4.80	20	3.182	s	4.15	11	3.77	1	3.80	22	4.6	2	4.65	15
3.49	3	3.95	42	2.940	ss	3.92	6	3.35	1	3.39	54	4.29	6	4.25	52
3.00	2	3.66	67	2.772	ww	3.72	75	3.18	10	3.20	47	3.99	7	4.02	52
2.77	8	3.52	27	2.623	w	3.35	12	3.03	<1	2.98	20	3.48	8	3.49	62
2.52	6	3.04	11	2.460	mw	3.22	84	2.94	<1	2.71	21	3.29	4	2.98	56
2.46	8	2.79	53	2.352	s	3.05	50	2.70	1	2.61	104	2.85	4	2.60	67
2.34	<1	2.52	60	2.265	ww	2.95	104	2.61	<1	2.56	20	2.59	10	2.40	19
2.27	5	2.47	78	2.173	mw	2.50	22	2.52	4	2.53	18	2.39	4	2.36	20
2.25	1	2.36	19	2.092	ms	2.37	55	2.35	4	2.37	18	2.26	2	2.20	16
2.163	2	2.33	14	2.052	m	2.33	11	2.22	1	2.22	8	2.19	4	2.13	12
2.032	<1	2.28	18	1.998	w	2.27	2	2.16	1	2.18	8	2.05	6	2.05	33
1.952	<1	2.26	17	1.933	w	2.21	10	2.08	<1	2.00	16	1.93	6	1.925	16
1.893	<1	2.166	14	1.850	ms	2.19	10	2.00	<1	1.96	16	1.90	4	1.880	11
1.749	8	2.049	7	1.807	w	2.11	55	1.93	5	1.945	21	1.86	4		
1.670	1	1.814	11	1.772	w	2.07	26	1.76	1	1.774	3	1.83	4		
1.640	<1	1.759	70	1.665	m	1.998	8	1.67	1	1.598	4	1.77	2		
1.620	1	1.749	44	1.610	mw	1.945	7	1.59	3	1.380	11	1.74	2		
1.573	<1	1.681	11	1.556	w	1.873	34	1.50	2			1.70	2		
1.498	2	1.648	46	1.522	m	1.863	6	1.47	2			1.66	8		
1.486	3	1.626	15	1.460	w	1.807	5	1.39	3			1.65	2		
1.436	<1	1.595	9	1.447	mw	1.787	2	1.37	8			1.598	7		
1.397	1	1.580	9	1.406	s	1.675	11	1.34	1			1.532	2		
1.350	2	1.508	20	1.392	s	1.626	11	1.34	1			1.510	6		
1.318	1	1.480	102	1.346	s	1.533	20	1.34	1			1.487	4		
		1.486	102			1.467	9					1.459	7		
		1.447	5			1.447	5								
		1.402	16			1.423	34								
		1.354	16			1.408	28								
		1.361	26			1.361	26								

TOXIC EFFECT OF VARIOUS DUSTS ON MONOCYTE

Talc			Pyrophyllite			Halloysite			Kibushiclay			Anthracite			Illite D			
B	No. 22			E	No. 23			D	No. 24			No. 25	No. 26			No. 27	No. 28	No. 29
	d	I	I		d	I	I		d	I	I		d	I	I			
9.4	80	9.4	190	9.14	40	9.2	217	7.2-7.5	8	7.14	129	14.3	23	10.3	77	10.0	10	
4.69	40	4.72	150	4.57	50	4.55	216					10.0	32	7.03	39			
		3.58	44	4.15	20							7.25	174	5.04	26	4.94	2	
3.88	1 b	3.75	27	3.87	5							5.04	13	4.46	34	4.47	9	
		3.12	211	3.34	30	3.40	8	4.42	10	4.46	63	4.27	17					
		2.75	36	3.037	100	3.06	225									3.68	2 b	
2.70	10	2.60	22	2.524	20			3.578	8	3.56	120	3.56	205	3.52	41			
2.59	20	2.48	40	2.400	40	2.41	5			3.33	65	3.35	91	3.34	52	3.32	9	
2.47	50	2.34	18	2.287	20	2.30	18							3.19	25	3.16	0.5	
2.32	10	2.22	18	2.142	15									3.03	26			
2.20	30	2.10	18	2.071	10			2.559	7					2.88	30	2.86	1	
2.09	20	1.869	50	2.044	10	1.845	25							2.60	6	2.60	6	
1.92	5			1.881	5									2.58	15	2.50	1	
1.86	30															2.41	4	
1.725	20	1.670	14	1.828	40			(2.48)	2							2.41	4	
				1.636	30			2.403	2									
1.67	40			1.621	15					2.36	33	2.38	70					
1.652	15			1.567	3					2.34	42							
1.632	1 b	1.558	22	1.522	10	1.537	5	(2.33)	1	1.994	14	2.00	20	2.02	14	1.982	1	
1.55	30	1.526	14	1.485	30													
1.52	40			1.463	5					1.670	23	1.791	35					
				1.432	5			1.800	1			1.664	10			1.689	3	
1.501	20			1.419	5			1.678	5							1.639	3	
1.461	10			1.377	40					1.540	13					1.53	6	
1.446	5			1.362	40			1.481	8	1.490	18	1.433	13					
1.405	20	1.397	20													1.446	0.5	
1.390	3 b															1.320	0.5	

FIBROGENIC ACTIVITY OF QUARTZ OF DIFFERENT SURFACE PROPERTIES

Hiroyuki SAKABE, Akira KAJITA and Kimiko KOSHI

In the previous paper Sakabe et al.¹⁾ studied the surface change of quartz particle by grinding and found the following.

- 1) After long time grinding, quartz particles lost their original sharp shape and became blunt, and some of the particles took the form of sphere or oval. But, these ground quartz particles recovered their sharp shape after the treatment with NaOH solution.
- 2) Initial dissolution velocity of quartz particles in NaOH solution or heated phosphoric acid solution increased with grinding time.
- 3) From the studies by means of X-ray diffraction, electron diffraction and infrared spectrum, it was assumed that the original surface structure of quartz particle was changed to take a disturbed and perhaps a random structure by grinding. These changes were intensified with the increase of grinding time. The modified surface layer of quartz particle produced by grinding disappeared, if the ground quartz particles were leached with NaOH solution.
- 4) The toxicity of quartz particles to the intraperitoneal monocytes decreased with the increase of grinding time.

In this paper, we should like to report the tissue reaction and some other biological reactions caused by various quartz particles of different grinding times in the experimental animals.

QUARTZ SAMPLES AND EXPERIMENTAL METHOD

Following samples of quartz particles were used in this experiment.

Q-I-2M.	Ishikawayama quartz particles ground for 2 minutes.
Q-I-6H.	" " " " " 6 hours.
Q-I-100H.	" " " " " 100 hours.
Q-I-L.	Q-I-6H treated with 10% NaOH solution.
Q-B-2M.	Brazilian quartz particles ground for 2 minutes.
Q-B-6H.	" " " " " 6 hours.
Q-B-L.	Q-B-6H treated with 10% NaOH solution.

These samples were prepared to have similar size distribution with a mean diameter of about 0.5μ by water elutriation. The details of preparation method were described in the previous paper.¹⁾

Nine male rats of Wister strain were injected with 1 cc of saline suspension of

FIBROGENIC ACTIVITY OF QUARTZ OF DIFFERENT SURFACE PROPERTIES

each of dust samples, in dose of 40 mg of quartz particles per animal. Rats were sacrificed at 1 month and 3 months after the injection.

Table 1 shows the animals which died spontaneously and were sacrificed. The lung sections fixed with formalin were stained with hematoxylin and eosin, Masson's

Table 1. Experimental animals and grade of fibrosis (albino rat)

	I-100H	I-6H	I-2M	I-L	B-6H	B-2M	B-L
Died spontaneously within 1 month after injection	No. 107	44	51	49			25
		46					45
							36
Sacrificed at 1 month after injection	108 (1)	42 (1)	4 (2)	56 (2-3)	2 (2)	1 (2-3)	47 (3)
	113 (1)	54 (1-2)	29 (2)	60 (3)	9 (1-2)	13 (1-2)	48 (2-3)
	114 (1)	58 (1)	50 (1-2)	65 (3)	22 (2)	15 (2)	53 (4)
	126(1)						
Died spontaneously during the 3rd month		12 (2)	63 (2)		30 (2)	43 (3)	
		20 (2)			32 (2)	62 (3)	
		55 (1)			34 (1)		
Sacrificed at 3 months after injection	111 (2)	3	8	18 (4)	7	11 (3)	10 (5)
	118 (2)	14	37 (3)	24 (4-5)	17 (4)	23 (2)	19 (5)
	125 (2)		40 (3)	26 (5)	31 (2)	39 (3)	52 (5)
	130 (1)		64 (3)	28 (5)		57 (3)	
				35			

Note: Intratracheal injection of quartz dusts was performed at 10, June, 1960, except I-100H which was injected at 5, September, 1960.

Figures in parentheses show the grade of lung fibrosis.

trichrome, and by silver impregnation. The degree of lung fibrosis was classified into five grades suggested by Belt and King²⁹.

EXPERIMENTAL RESULTS

Death of animals. Within 1 month after injection, 7 animals died spontaneously. Experimental groups of these animals are shown in Table 1. Their survival days after injection were 5, 8, and 8 days in Q-B-L group, 6 days in Q-I-L, 4 days in Q-I-2M, 11 and 24 days in Q-I-6H, and 15 days in Q-I-100H.

Early death of animals in Q-B-L, Q-I-L and Q-I-2M groups were assumed to be related to the severity of tissue reaction, because the more progressed fibrosis of the lungs was observed afterwards in these groups than in the other ones. The cause of later death of 9 rats was assumed to be infections.

Change of body weight. The change of mean body weight in each group after injection is shown in Fig. 1 and 2. Eight animals which died spontaneously were excluded from the calculation of mean value. All animals showed the decrease of

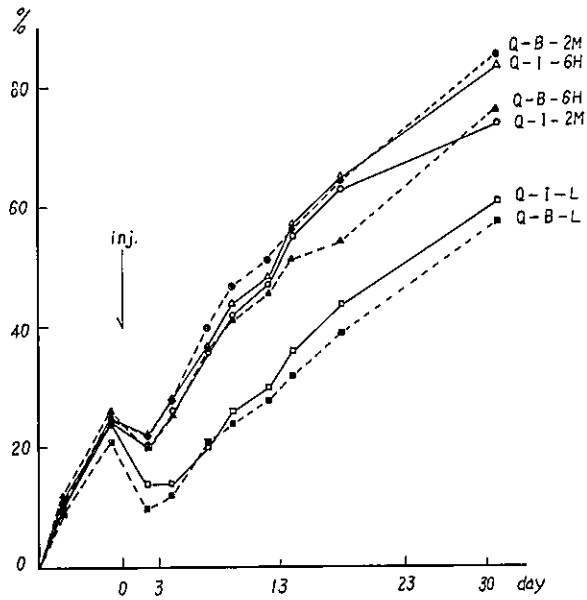


Fig. 1. Decrease and recovery of body weight after intratracheal quartz injection.

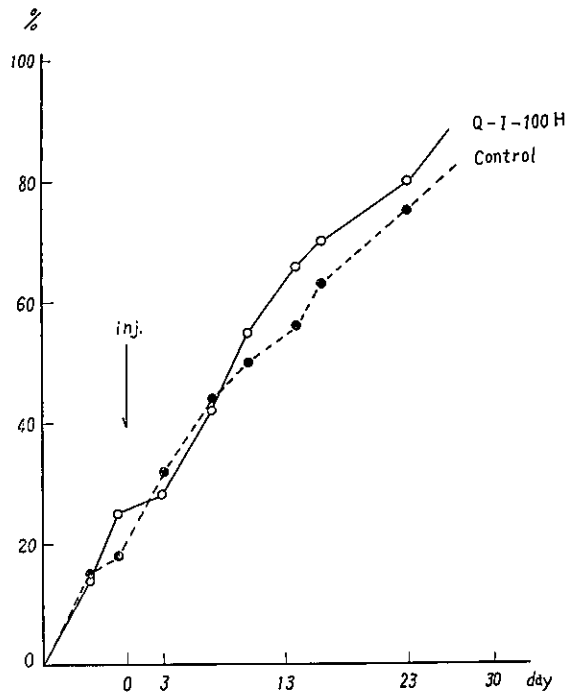


Fig. 2. Decrease and recovery of body weight after intratracheal quartz injection.

FIBROGENIC ACTIVITY OF QUARTZ OF DIFFERENT SURFACE PROPERTIES

weight soon after the injection except Q-I-100H group. The most remarkable decrease was observed in Q-B-L and Q-I-L groups, moderate decrease in Q-I-2M, Q-I-6H, Q-B-2M, and Q-B-6H groups, and no decrease in Q-I-100H. Recovery of weight after the decrease and the rate of weight gaining were slow in Q-B-L and Q-I-L groups.

Gross appearance of the lung. The grade of macroscopical change of the lungs was assessed from the spread of nodules. Severity of the lung change in each group at 1 month after injection increased in the order Q-I-100 H < Q-I-6 H < Q-I-2 M < Q-I-L in Ishikawayama quartz and Q-B-2 M < Q-B-6 H < Q-B-L in Brazilian quartz. The same order was also observed at 3 months.

Wet weight of the lungs with heart. After the animals were killed with ether, the lungs and heart were weighed together. The ratios of wet weights of the lungs with hearts to body weights at 3 months after the injection are illustrated in Fig. 3.

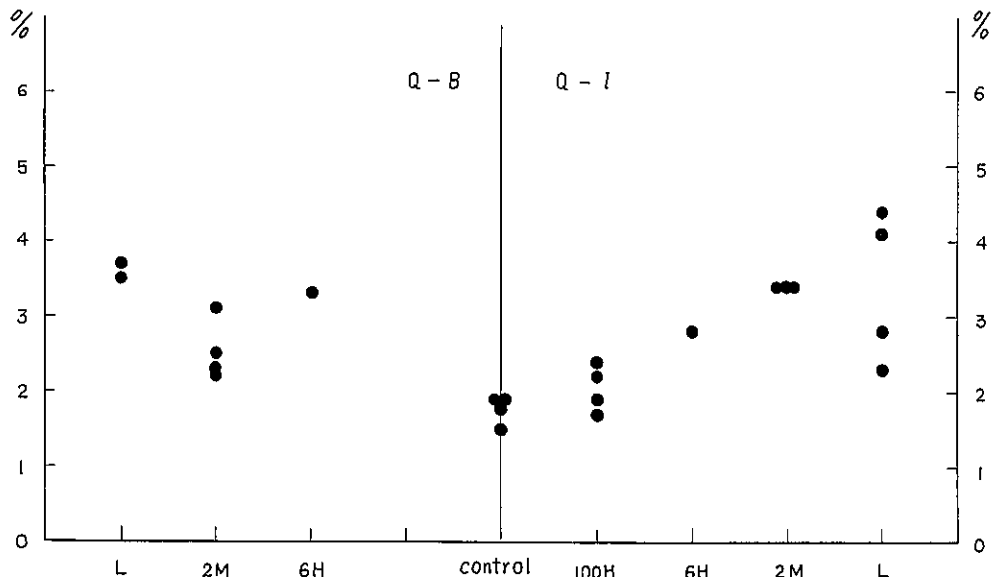


Fig. 3. The weight of lungs with heart of rats injected various quartz.
 Note: Organs weights are shown in percentage to body weight.

Lung weights of animals in each group were assumed to show a tendency to increase in the order Q-I-100 H < Q-I-6 H < Q-I-2 M < Q-I-L, and Q-B-2 M < Q-B-6 H < Q-B-L, although the number of survived animals were few.

Fibrosis of the lungs. Grades of fibrosis of animals are shown in Table 1 and summarized in Table 2. Lung fibrosis was developed most rapidly in the animals of Q-B-L and Q-I-L groups. The most weak fibrosis was obtained with Q-I-100 H. Average grades of fibrosis in Q-I-6 H and Q-B-6 H groups were not determined, as the survived animals were too few. However, if we consider including the animals

Table 2. Histological changes produced in the lungs of rats by various quartz dusts. (grade of fibrosis by King)

	I-100H	I-6H	I-2M	I-L	B-6H	B-2M	B-L
At 1 month after injection	1	1	2	3	2	2	3
At 3 months after injection	2		3	5		3	5

that died spontaneously, fibrogenic activity up to 3 months increased in the order Q-100 H < Q-6 H, Q-2 M < Q-L. No distinctive difference was found between Ishikawayama and Brazilian quartz.

With regard to the pathological changes in lymph gland, it must be noted that Q-I-100 H produced the enlargement and fairly developed fibrosis of the mediastinal lymph glands, while it proved to be least effective in fibrosis production in the lung among quartz samples.

DISCUSSION

Normal weight gaining of rats was disturbed temporarily after the intratracheal injection of various quartz particles except 100 hours ground quartz. The most remarkable decrease of weight was observed in the group injected with NaOH treated quartz. Effect of 2 minutes or 6 hours ground quartz on body weight was stronger than 100 hours ground quartz and weaker than NaOH treated quartz. It is assumed that the loss in body weight after quartz injection is caused by the lung damage and its degree depends upon the severity of the tissue reaction, although other complicated biological reactions can not be neglected.

Quartz samples showed the same order of fibrogenic potency as the inhibitory effect to the body weight, that is, NaOH treated quartz produced the most developed fibrosis, 100 hours ground quartz the weakest, and the other two sorts of quartz produced the reaction of the grade between these two samples. The similar relation was also observed in the lung weight.

From these results obtained in this short period experiment, initial velocity of the fibrosis development by quartz samples used in this experiment seems to increase in the order Q-100 H < Q-6 H, Q-2 M < Q-L. And, from general impression, it seems that Q-2 M has a little stronger effect than Q-6 H.

Toxic effect of these quartz to the monocytes in vitro increased in the order Q-100 H < Q-6 H < Q-2 M < Q-L as reported in the previous paper.¹⁾ Therefore, it is assumed that the intensity of cell toxicity of these quartz dusts may be roughly

FIBROGENIC ACTIVITY OF QUARTZ OF DIFFERENT SURFACE PROPERTIES

correlated to their fibrogenic potency, in other words, quartz dust of severe cell toxicity produces a well developed fibrosis in the lungs of rats in a short period.

It must be noticed that the difference of intensity between the neighbouring two quartz samples in the series of the order of cell toxicity was definite, but it is not so clear in the fibrogenic potency series except Q-L which has a distinguished activity. This may be explained by the assumption that fibrosis is a far more complicated biological reaction as compared with the cell damage in vitro. However, if the modified surface layer of quartz particles is dissolved away in the cell or tissue, dissolution velocity may participate in this problem. Experimental results obtained in our studies suggest strongly that the trigger of the process of collagen formation by quartz in the lungs may be the phagocytic cell damage which is caused by the surface of ingested quartz particle.

On the other hand, it must not be overlooked that the silicotic nodule which is seen in human lungs and composed of collagen strands arranged in the form of whorl was never produced in experimental animals. Sano⁹⁾ reported that the experimental lung fibrosis by quartz is the result of alveolitis which is not seen in human silicosis. In this study, too, it may be supposed that the fibrosis of rat's lungs is the result of alveolitis caused by alveolar cell damage. At present, it seems difficult to explain the difference of collagen arrangement of the silicotic nodule between man and animal. As far as concerning the experimental silicosis, however, cell toxicity of quartz seems to play the most important role in the fibrosis development.

SUMMARY

Tissue reaction and some other biological reactions produced by various quartz particles of different surfaces, were studied and the results were compared with cell toxicity. The most developed lung fibrosis of rats was obtained by NaOH treated quartz and the least by quartz ground for 100 hours. Quartz ground for 2 minutes or 6 hours produced the fibrosis of the grade between above two samples. This order in fibrogenic potency of these quartz held good in cell toxicity and in effect on body weight. Phagocytic cell damage which is caused by the surface of ingested quartz particle may be a trigger of the process of collagen formation by quartz in the experimental animals.

Grateful acknowledgement was due to competent assistance by Miss S. Shimizu in our laboratory.

REFERENCES

- 1) Sakabe, H., Kawai, K., Koshi, K., Soda, R., Hamada, A., Shimazu, M. and Hayashi, H. : Bull. Nat. Inst. Industr. Health, 4, 1, (1960).
- 2) Belt, T.H. and King, E.J.: Report 250, Medical Research Council, Special Report

Series, (1945).

3) Sano, T. and Osanai, H.: Report of the Institute for Science of Labor, 55, 27, (1959).

要 旨

表面性状の異なる各種石英粉末の線維増殖能

坂 部 弘 之 梶 田 昭 興 貴 美 子

石英粉末の表面の物理化学的性質は粉末を作製する時の条件，特に磨砕時間により異なること及び表面の性状を異にする石英粒子は，試験管内で培養した単核細胞に対する毒性においても相違を示すことを前報において報告したが，本研究では，このような石英粒子をラットの気管内に注入し，ラット体重の推移，及び1ヶ月，3ヶ月後における，肺線維症の発達の程度をしらべた。

実験に使用した石英は，ブラジル産及び，石川山産石英の2分間磨砕，6時間磨砕，アルカリ処理のものと石川山産石英の100時間磨砕のものである。これらの石英をそれぞれの時間磨砕した後，又はアルカリ処理した後に，水ひにより平均粒径 0.5μ のものを集めて実験に使用した。この実験の結果判ったことは，

- (1) 石川山産とブラジル産の両石英の間には線維増殖能に著しい差は見出されなかった。
- (2) 100時間磨砕の石英の線維形成能は最も弱く，アルカリ処理石英は圧倒的に強い線維形成能をもち，2分間磨砕，6時間磨砕のものは，その中間に位した。
- (3) 石英粉末気管内注入直後，ラット体重の一時的減少が見られた。各種石英粉末による体重減少度と，それらの線維増殖能との間には相関があり，アルカリ処理石英を注入された動物の体重減少が最も著明であり，100時間磨砕のものでは，体重減少は見られなかった。
- (4) 以上の結果を，前報に述べたそれぞれの石英粒子のもつ細胞毒性和対比してみると，大体相関し，細胞毒性の高い石英粒子程線維形成能も強かった。

従って，石英粉末を実験動物の気管内に注入することによりひきおこされる，膠原線維形成において，石英粉末を摂取した食細胞が障害されるということは，極めて重要な意義をもつものと思う。即ち，肺組織内に侵入した石英粉末を摂取した食細胞の障害の程度が，爾後の膠原線維形成に迄至る一連の組織反応を強力に支配するものと思う。

DETERMINATION OF MIST SIZE BY METAL COATED GLASS SLIDE

Hisato HAYASHI, Shigeji KOSHI and Hiroyuki SAKABE

There is much need of the determination of size and numbers of mist in the field of industrial hygiene as well as air pollution research. For this purpose, the method of Gerhard and Johnstone (1955)¹⁾ or of Lodge and Fanzoi (1954)²⁾ has been used as the reliable technique. Recently, Lodge, Ferguson and Havlik (1960)³⁾ reported a new method, which was obtained by combining above two methods. For the size determination of sulfuric acid mist, the authors used these three methods, but could not get any satisfactory result, as the reaction spot on the gelatinous film changed its size by absorbing moisture in the air. Therefore, the authors have developed a new method which is not affected by humidity in the air and determined the size of acid and alkaline mist by the new method.

EXPERIMENTAL RESULTS AND DISCUSSION

According to our new method, mist was caught on a metal coated glass slide. The slide is prepared as follows: a slide glass was placed in a vacuum evaporator at an angle of 14° and at a distance of 140 mm from tungsten filament and then approximately 30 mg of metal was evaporated in vacuum. As metal, iron, copper, aluminium or other metals were used. After the treatment, glass slide was found to be covered with very thin layer of metal film. For the collection of mist particles, Owens type dust counter or cascade impactor were employed, and the metal coated glass slide was inserted in these collector as collecting plate instead of ordinary non-treated glass slide.

Mist was generated from an atomizer, which ejected air through very fine nozzle against the surface of aqueous solution of the acid and alkali. In the experiment the ratio of 1:1 H_2SO_4 , 1:10 H_2SO_4 , 1:1 HCl and 1:10 HCl solutions were used. Five or ten percent of NaOH solutions were used as alkaline one.

When the acidic mist was deposited on this metal coated glass slide, metal was dissolved away, and there remained transparent holes corresponding to the sizes of the mist. Thus the reaction spot was obtained as a transparent hole. Fig. 1 illustrates these holes. Therefore, the reaction between the size of hole and true size of mist was investigated. The determination of true size of acid mist was carried out by catching mist particles in nujol layer on the glass slide. Mist particles in this nujol layer were assumed to give true size, since the particles were suspended

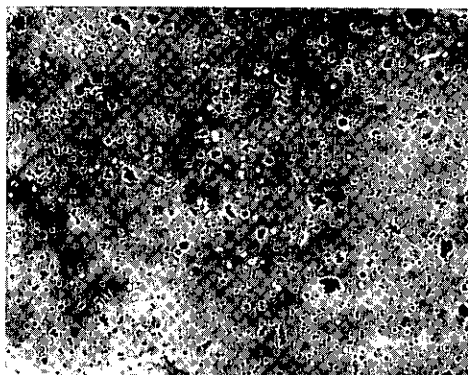


Fig. 1. Reaction spots of sulfuric acid mist on iron coated glass slide. Spots are the holes in which iron was dissolved away.

in nujol.

As for 1:1 H_2SO_4 mist, the cumulative distribution curves of diameters of droplets (D) in the nujol, and reaction spots (d) on the iron coated glass slide are shown in Fig. 2. In this Fig. 2, the cumulative distribution curve of $d^{\frac{2}{3}}$ is also indicated. The shape of the curve of $d^{\frac{2}{3}}$ is resemble closely to that of the curve D. As the diameter of reaction spot increased with reaction time absorbing the moisture in the air, the change of size with reaction time was examined for mist and iron film at 0, 1, 2, 3, 4 and 5 minutes respectively after sampling. After reaction has continued for above each time, the iron coated glass slide was rinsed with alcohol to stop further reaction, and the slide was examined under an optical

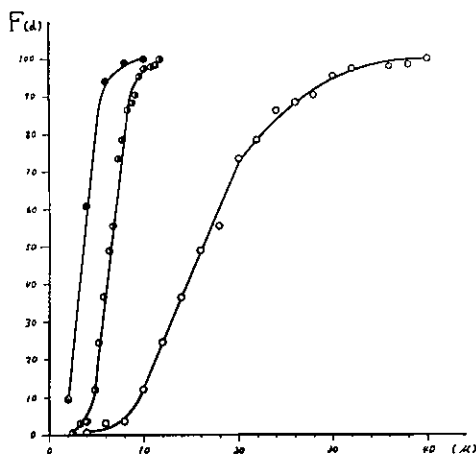


Fig. 2. Cumulative size distribution curves of sulfuric acid mist. Note: Cumulative distribution curves of the diameter of droplets in nujol (●), of reaction spot diameter (d) on iron coated glass slide (○), and of $d^{\frac{2}{3}}$ (●).

DETERMINATION OF MIST SIZE BY METAL COATED GLASS SLIDE

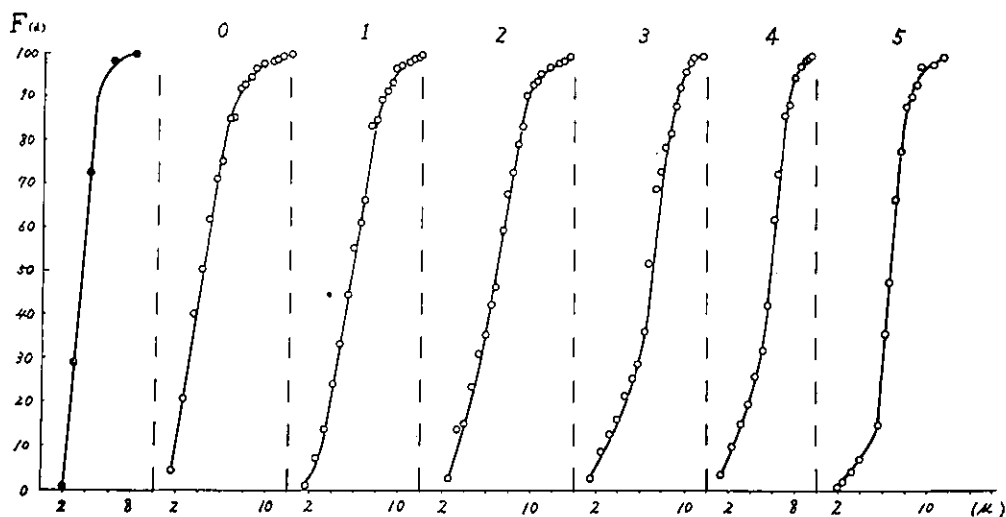


Fig. 3. Cumulative size distribution curves of sulfuric acid mist.

Note: The left side curve (●) shows the diameter of mist droplets in nujol. The other curves (0, 1, 2, 3, 4, and 5) exhibit the measured diameter d raised to the $2/3$ power ($d^{2/3}$) of the reaction spot of mist on the iron coated glass slide. Curve number shows the minutes of reaction time, for example, curve 3 was obtained from the slide rinsed with alcohol at 3 minutes after sampling.

microscope. The cumulative distribution curves of $d^{2/3}$ from 6 samples ($d_0^{2/3}$, $d_1^{2/3}$, $d_5^{2/3}$) are shown in Fig. 3. As presented in Fig. 3, shape of these curves obtained after three or more minutes are quite similar to the curve D of the same mist particles in nujol except the range of very small size. From this result, reaction time of five minutes film may be suitable to obtain the true size. In the experiment, the metal film was reacted with mists for five minutes, and rinsed with alcohol.

To examine the effect of acid concentration of the mist on the hole size, the mists of 1 : 1 H_2SO_4 and 1 : 10 H_2SO_4 were collected on the iron or copper coated glass slide. After standing 5 minutes, the metal coated glass slide was rinsed with alcohol, and then dried by drier. Each cumulative distribution curve of $d^{2/3}$ is shown in Fig. 4. The shapes of these curves are similar to that of the cumulative distribution curve of droplets in the nujol.

In the case of the mists of 1 : 1 HCl and 1 : 10 HCl, the cumulative distribution curves of $d^{2/3}$ obtained from reaction spots on the iron and copper coated glass slide were in a similar fashion. As seen in Fig. 5, the shapes of the curves of $d^{2/3}$ are similar to that of the droplets size in the nujol.

Concerning the metals used to cover the surface of glass slide, iron was most suitable for the mists of H_2SO_4 and HCl solutions as far as we have attempted. Some interesting facts were found in the metal coated glass slides on which mists deposited when the slides were left without rinsing with alcohol. That is, crystal

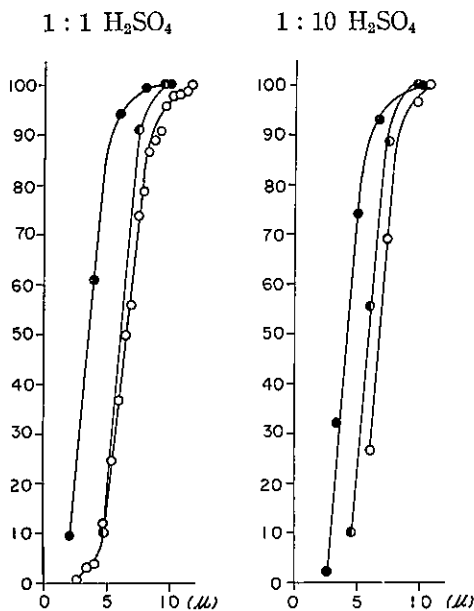


Fig. 4. Cumulative distribution curves of 1 : 1 H₂SO₄ mist (left) and 1 : 10 H₂SO₄ mist (right)

Note : 1) cumulative distribution curves of droplet size in nujol (●), of d_{Fe}^2 of reaction spots (d_{Fe}) on iron coated glass slide (○), and of d_C^2 of reaction spots (d_C) on copper coated glass slide (●). 2) (d) means the diameter of reaction spot measured directly on the metal coated glass slide.

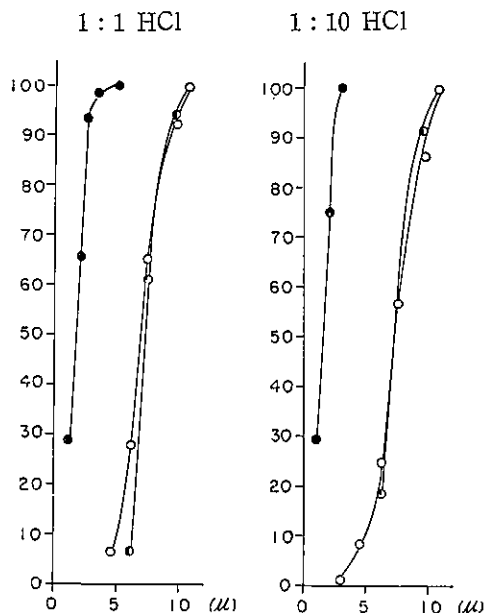


Fig. 5. Cumulative distribution curves of 1 : 1 HCl mist (left) and 1 : 10 HCl mist (right)

Note : 1) cumulative distribution curves of droplet size in nujol (●), of d_{Fe}^2 of reaction spots (d_{Fe}) on iron coated glass slide (○), and of d_C^2 of reaction spots (d_C) on copper coated glass slide (●). 2) (d) means the diameter of reaction spot measured directly on the metal coated glass slide.

was formed by the chemical reaction of acid with metal. By microscopical observation of this crystal, the chemical composition of unknown mist may be elucidated.

In the case of alkaline mist, the mists of 5 % and 10 % NaOH solutions were collected on aluminium coated glass slide in the same way. The cumulative distribution curves of d^2 obtained from the reaction spot on the slide are shown in Fig. 6. The shapes of these curves are also similar to that of cumulative distribution curves of the diameter of droplets in the nujol.

From these experiments, it is clear that the cumulative distribution curve of d^2 obtained from reaction spots on the metal coated glass slide shows the same shape as that of the diameter (D) obtained from the natural mist droplet, if the size of mist particle suspended in nujol is assumed to be the same as that of particles suspended in air. Then the cumulative distribution curve of d^2 may be easily shifted to the curve of D by the following experimental relationship.

$$D = ad^{\frac{2}{3}} - b$$

DETERMEINATION OF MIST SIZE BY METAL COATED GLASS SLIDE

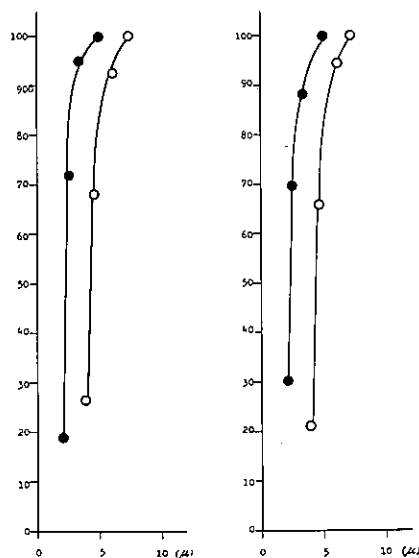


Fig. 6. Cumulative size distribution curves of 10% HaOH mist (left) and 5% NaOH mist (right).

Note: cumulative size distribution curves of droplets in nujol (●), and of d_{SA}^2 in which was the directly measured size of reaction spots on aluminium coated glass slide. (○)

where d is the diameter of reaction spot on the metal coated glass slide, and values of a or b are shown in table 1.

Table 1. Relationship between mists and a or b in experimental equation

mists	metal	a	b	
H ₂ SO ₄	1 : 1	iron	0.8	1.7
	1 : 10	iron	0.9	2.2
	1 : 1	copper	1	3.6
	1 : 10	copper	0.5	-1.6
HCl	1 : 1	iron	0.5	2.6
	1 : 10	iron	0.6	3.1
	1 : 1	copper	1.1	-0.8
	1 : 10	copper	0.6	3.1
NaOH	5%	aluminium	1	1.9
	10%	aluminium	1	2

The value of transforming factor must become constant, because of the shape of cumulative distribution curve of d_{SA}^2 is similar to that of D. The copper coated glass slide is not suitable for size determination of acid mist, as it has variable value of transforming factor. Therefore the selection of the metal which was used to coat on the slide must be chosen from many metals under the consideration of the properties of the mist.

FIELD TEST PERFORMED APPLYING THIS METHOD

The size of sulfuric acid mists generated from electrolysis process in a certain plant was determined by this method. Sulfuric acid mist was collected on iron coated glass slide by cascade impactor. The cumulative distribution curve of d was drawn from the size of the sulfuric acid mist measured. The true diameter of droplets of the sulfuric acid mist was obtained from the experimental equation (1), substituting average of upper two values of each column (a) and (b). Results are shown in Fig. 7.

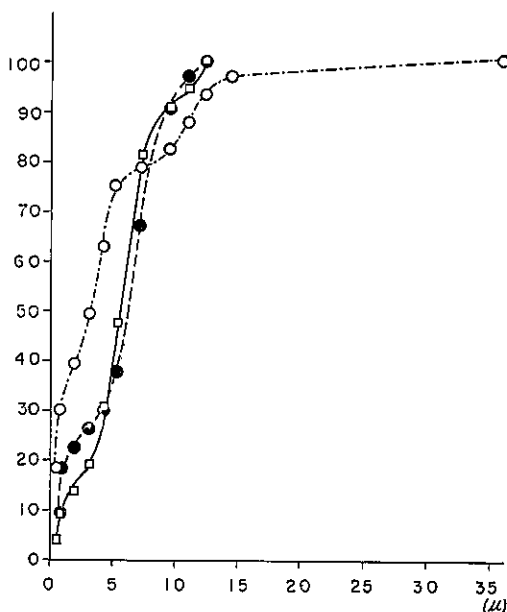


Fig. 7. Cumulative size distribution curves of sulfuric acid mist from electrolytic cell.

Note: Just above electrolytic cell (O), above 1 meter from electrolytic cell (●), in path of both electrolytic cell (□).

This method is also available in air pollution research. Particles were collected on the iron coated glass slide by cascade impactor. In this case, sometimes reaction spots were not shortly after sampling, but if these slides were exposed to the condition of high humidity for enough time, spots appeared independently or around the solid particles. These phenomena may be explained by the hygroscopic acid mist or hygroscopic solid particle.

SUMMARY

New method for the determination of the size of acid or alkaline mist was carried

DETERMINATION OF MIST SIZE BY METAL COATED GLASS SLIDE

out. Mist was collected on the metal coated glass slide. At five minutes after sampling, test slide was rinsed with alcohol. Thereafter the size of reaction spot on the metal coated glass slide was measured. The method of calculating the true size of mist was described.

This method is very convenient for the determination of size and number of acid and alkali mist, as it is very simple and not affected by moisture.

REFERENCES

- 1) Gerhard, E. R. and Johnstone, H. F.: Anal. Chem. 27, 702-703, (1955).
- 2) Lodge, J. P. and Fanzoi, H.: Anal. Chem. 26, 1829, (1954).
- 3) Lodge, J. P., Ferguson, J. and Havlik, B. R.: Anal. Chem. 32, 1206-1207, (1960).

要 旨

ミ ス ト の 粒 度 の 測 定

林 久 人 興 重 治 坂 部 弘 之

電気分解, メッキ, 表面汚染除去などの工程において発生する酸アルカリのミストの粒度を知ること, その生物学的作用の理解のために, またその対策のために必要である。しかしミストの粒度と数の測定は, 酸・アルカリのミストの粒度が空気中の水分を吸収して大きくなるので, その測定は非常に困難である。

筆者等はミストの粒度の測定のために, 電子顕微鏡の試料を製作する時に使用するベルジャーを用いて金属の被膜をカバーガラス, またはガラス板上に蒸着したのものの上にミストを捕集すると, 金属は溶けて, ミストの粒度に比例した透明な痕跡が残る。(第1図)

スライド上の薄い流動パラフィン層中にミストを捕集したものが, 真の粒度を持つと仮定してミストの粒度と痕跡の大きさとの関係を調べた。第2図に, 流動パラフィン中に捕集した1:1硫酸ミストの累積分布曲線(1)と, 鉄の被膜上に1:1硫酸ミストを捕集し, その被膜上の痕跡の直径の累積分布曲線(2)と, 痕跡の直径の $2/3$ 乗の累積分布曲線(3)を示す。(1)と(3)の曲線の形は非常に良く類似する。

次に鉄の被膜上に1:1硫酸ミストを捕集し0, 1, 2, 3, 4, 5分後にアルコールで洗滌し, 被膜上の痕跡の直径の $2/3$ 乗の累積分布曲線を第3図に示した。結果をみると, ミストを流動パラフィン中に捕集して作った累積分布曲線の形と, 捕集後3~5分後にアルコール洗滌したスライドの, 被膜上の痕跡の直径の $2/3$ 乗の累積分布曲線の形とは非常に小さい粒度範囲を除いて類似する。この実験では, ミストの捕集後5分経過したスライドをアルコール洗滌し, 金属の被膜上の痕跡の直径の $2/3$ 乗の累積分布曲線を作った。

上述の方法で, 鉄または銅の被膜上に捕集した1:1硫酸, 1:10硫酸ミストの累積分布曲線を第4図に, 1:1塩酸, 1:10塩酸ミストの累積分布曲線を第5図に5%と10%苛性ソーダのミストをアルミニウムの被膜上に捕集し, その痕跡の直径の $2/3$ 乗の累積分布曲線を第6図

に示した。

多くの実験の結果から、金属の被膜上に捕集したミストの痕跡の直径の $2/3$ 乗の累積分布曲線と真のミストの粒度の累積分布曲線から真のミストの直径を求めると

$$D = ad^{3/2} - b$$

となる。

但し、 d は金属の被膜上のミストの痕跡の直径、 a と b とは第一表を参照。

銅の被膜上に硫酸、塩酸のミストを捕集し真のミストの直径を求める場合に係数が一定しないので銅の被膜は不適當である。実験の結果から、真のミストの直径を求めるに適當な金属は酸ミストの場合には鉄、苛性ソーダのミストの場合にはアルミニウムである。この様にガラススライドを被覆する金属はミストの性質を考慮して選択する必要がある。

ここに確立された方法は、金属の被膜をカバーガラスまたはガラス板上に蒸着したものの上にミストを捕集し、反応時間 5 分後にこれをアルコールで洗い、金属の被膜上の痕跡の直径の $2/3$ 乗の累積分布曲線を求め、この分布曲線と真のミストの粒度の累積分布曲線からミストの粒度と数を比較的容易に求めることが出来る。

この方法を利用して、某工場の電気分解槽より発生する硫酸ミストの粒度分布を測定し、その結果を第 7 図に示した。この方法は比較的簡単であり、かつ精度が良いので、ミストの粒度および個数の測定が必要な時に広く使用されることが考えられる。

また、この方法を応用して、大気中の SO_2 、その他の酸性の吸水性物質についても同様な結果を得た。

EXPERIMENTAL STUDY ON APPLICATION OF STRAIN GAGE TO ACCELEROMETER.

Toshisuke MIWA

Recently, the use of vibrating tool has been increased in industry and many papers¹⁾ have been reported the problems concerning with the health hazards caused by vibration in the field of the industrial hygiene. However, the correct measurement of vibration is so difficult that there are still many problems which have to be solved in the future. These difficulties may include the following items.

1) If an accelerometer is not attached tightly to vibrating objects, the measurement can not be carried out rightly. Therefore, the fixation of the instrument is important especially to measure large accelerations or pulsive vibrations.

2) If the mass of the accelerometer is not considerably less than that of the vibrating system, the system may be disturbed by the fixing accelerometer.

3) If the main component of the vibration vector is not chosen, the vibration can not be measured correctly, because the vibration is the vector in three dimensions.

To overcome these difficulties, the accelerometer made of Barium Titanate may be useful. However, as this accelerometer has a capacitive impedance, it must be used with the preamplifier of considerably high input impedance. Moreover, the lower the frequency of vibration the higher is the impedance of the preamplifier. So, the accelerometer of this type is inconvenient to measure the vibration of the low frequency. In order to avoid the inconvenience, the author attempted to make use of the semiconductor strain gage, because of its easiness to amplify the output of the gage and of its having sufficient sensitivity to even the static displacement.

To meet the demand in the field of industrial hygiene, the accelerometer needs to satisfy the following conditions: (1) linear sensitivity to the acceleration from $10^{-3}g$ to $10g$, (2) wide frequency band from 0 to $10kc$, (3) ability to pick up the pulsive vibration as well as the sinusoidal one, and (4) easiness to screw the accelerometer upon the vibrating systems.

Only one type of accelerometer can not satisfy above conditions simultaneously. Therefore, the cantilever beam type was selected among many kind of accelerometers. The reason why the instrument was selected is due to the facilities to suit above conditions by choosing the beam's length, width and thickness variously and to deduce the characteristics of the beam from the vibration theory. However, the instrument was not adequate for the measurement of the vibration above $1kc$, because in the range over $1kc$ the strain of cantilever's arm was too little for the strain gage to sense.

The present paper deals with the construction of the accelerometer which has the natural frequency over 2 kc and sensitivity from 1 g to 200g and of the amplifier of the gage with the aid of transistors.

THEORY OF ACCELEROMETER.

According to the vibration theory²⁾ in connection with Fig 1, the following equation could be deduced

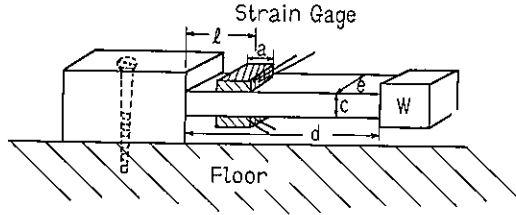


Fig. 1. Accelerometer making use of cantilever.

$$\frac{\xi_m}{y_m} = \frac{1}{\left(\frac{\omega_n}{\omega}\right)^2 - 1} \quad (1)$$

The symbols in Eq. (1) are defined as: ξ_m = maximum relative displacement between the floor and the lumped weight W , y_m = maximum displacement of the floor itself, ω = angular frequency of the sinusoidal vibration of the floor, ω_n = natural frequency of the cantilever. In the case of this cantilever beam with the distributed weight, ω_n is written as follows²⁾,

$$\omega_n = \frac{\pi^2}{4} \sqrt{\frac{\alpha}{0.454\alpha + 2}} \sqrt{\frac{EIg}{wd^4}}$$

where $\alpha = \frac{wd}{W}$, $I = \frac{ec^3}{12}$, E = Young's modulus, $g = 980 \text{ cm/sec}^2$, w = distributed weight of its arm of unit length, W = lumped weight.

When the strain gage with the length "a" is applied at the distance "l" from the clamped end of the arm as shown in Fig. 1, the maximum mean strain over gage's length (ρ_m) with respect to the maximum displacement of the lumped weight is shown in the following equation (2),

$$\rho_m = G\xi_m \quad (2)$$

where G is the function of "a", "l" and adhesive used for cementing the strain gage upon the cantilever and is decided experimentally. Therefore, its maximum strain against the maximum displacement of the floor is denoted in equation (3),

$$\frac{\rho_m}{y_m} = G \frac{1}{\left(\frac{\omega_n}{\omega}\right)^2 - 1} \quad (3)$$

EXPERIMENTAL STUDY ON APPLICATION OF STRAIN GAGE TO ACCELEROMETER

MEASUREMENT OF SENSITIVITY OF ACCELEROMETER

Measurement of sensitivity of accelerometer was divided into two parts by the frequency range. The first part was within the frequency range of 5–50 c/s and the second part 50–500 c/s, as the pen writing recorder works only under 50 c/s.

(I) The accelerometer was attached tightly to the vibration exciter. Then, keeping the acceleration amplitude of exciter constant and changing the frequency from 5 to 50 c/s, the out put of the strain gage amplifier was recorded by the pen writing recorder as shown in Fig (2).

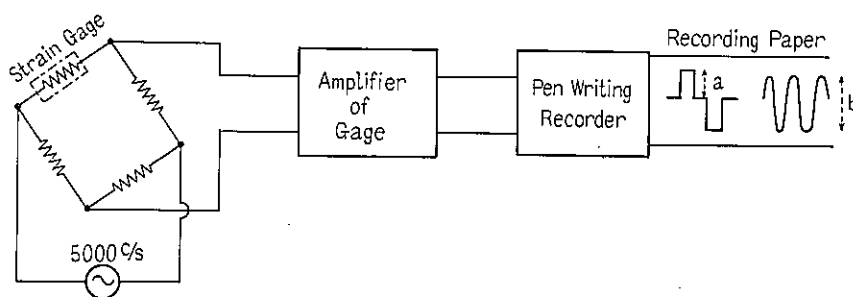


Fig. 2. Calibration of accelerometer within the frequency range of 5–50 c/s.

(II) In the frequency range from 50 to 500 c/s, its out put was connected as shown in Fig (3). Amplifier (1) and (2) were adjusted to give moderate value to

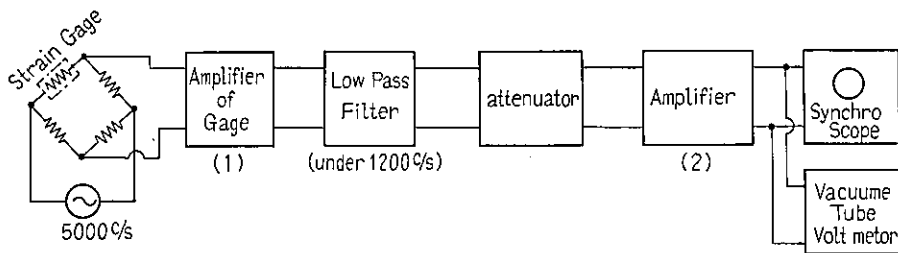


Fig. 3. Calibration of accelerometer within the frequency range of 50–500 c/s.

the vacuum tube voltmeter. Then, driving the exciter as described in (I) and changing the frequency, the attenuator was adjusted to make the same reading as the value at 50 c/s to the V.V. The difference between attenuator values at 50 c/s and some other frequency was obtained.

In these cases, the amplitude of the exciter table was calibrated by the microscope of 100 magnifications. The average value of amplitudes at the edges of opposite sides of the table was used to avoid the rocking. The magnification of the microscope was estimated by the graduated object glass and the frequency measurement was done by Lissajous' figure. The sensitivity measurement over 500 c/s was not tried

in this time because of difficulties involved in measurement of the amplitude by this microscope.

Then, the acceleration expressed as the unit of $g=980 \text{ cm/s}^2$ is as follows,

$$\frac{a}{2} \omega^2 / 980$$

where ω = angular frequency of the sinusoidal vibration of the table and "a" = its peak to peak amplitude in cm. The sensitivity of the accelerometer was calculated in Eq. (4),

$$k = 20 \log \frac{\frac{e}{e_0}}{\alpha} \dots\dots\dots (4)$$

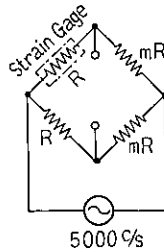


Fig. 4. Constituent elements of strain gage bridge.

In this equation, α = acceleration of the table measured with the unit of g , e = open circuit voltage of the gage applied to the accelerometer fixed on the table and e_0 = m. volt.

When the calibration signal corresponding with static strain, $s=5 \times 10^{-6}$, was fed into the bridge, e_1 was out put voltage of the latter and "a" was the amplitude in recording paper corresponding with this signal. When the exciter was driving the accelerometer, the out put voltage of the gage was expressed as e_2 and the peak to peak amplitude in the paper was "b" in this case. This is shown in Fig (2) and Eq. (5) was obtained

$$e_2 = e_1 \left(\frac{b}{2a} \right) \dots\dots\dots (5)$$

On the other hand, Eq. (6) was derived by the theory of the strain gage^{4,5,6)},

$$e_1 = SFE \frac{m}{(m+1)^2} \dots\dots\dots (6)$$

where F = gage factor and E = A. C. voltage fed into the bridge and m = the magnification factor of the bridge as shown in Fig. (4). Therefore, Eq. (7) was obtained from Eq. (4), (5), and (6).

$$k(db) = 20 \log S + 20 \log F + 20 \log E + 20 \log \frac{m}{(m+1)^2} + 20 \log \frac{b}{a} + 54 - 20 \log \alpha \dots (7)$$

EXPERIMENTAL STUDY ON APPLICATION OF STRAIN GAGE TO ACCELEROMETER

RESULTS

In the first place, the experiment was designed to examine the practical fitness of the Eq. (3) and Eq. (7) by the use of cantilever type accelerometer having common wire strain gage. For this purpose, the author constructed a new cantilever type accelerometer, which is made of phosphor bronze (specific gravity $s=8.72$ Young's modulus $E=4.07 \times 10^6$ kg/cm²) and has the theoretical natural frequency of 82.5 c/s as shown in Fig 5a. Employing this instrument, the author could get satisfactory agreement between the sensitivity of accelerometer and experimental Eq. (3) and (7) as shown in Fig 5b, only when the measuring value of 20 c/s was substituted for the value of G in the equation.

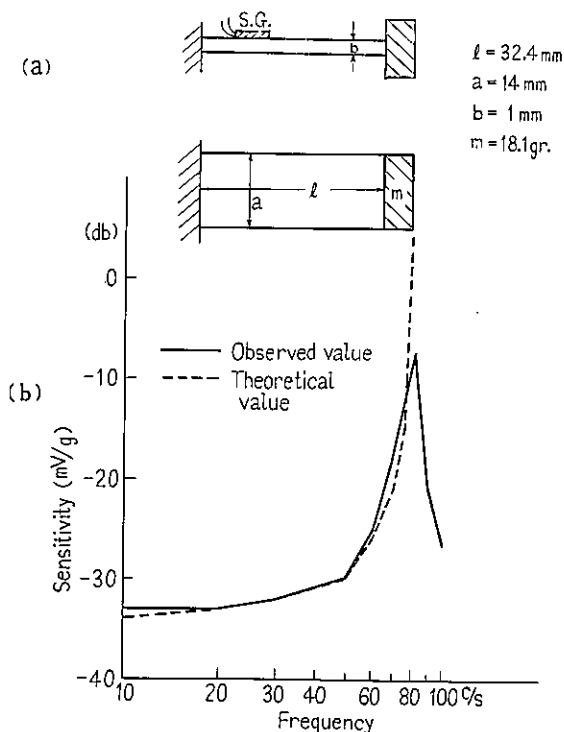


Fig. 5. Experimental proof of Eq, (3).

- a) Accelerometer of cantilever type with common wire strain gage. The accelerometer is made of phosphor bronze, (specific gravity $s=8.72$, Young's modulus $E=4.07 \times 10^6$ kg/cm²) and its theoretical resonance frequency is 82.5 c/s.
- b) Frequency characteristics of sensitivity, db in unit mV/g. G in Eq. (3) is corresponded with the measuring value at 20 c/s.

In the second place, in order to apply the above facts to practical measurement of vibrations, the accelerometer of phosphor bronze having two semiconductor gage

was prepared as indicated in Fig 6a. High sensitivity of accelerometer could be obtained by the use of the semiconductor strain gage, for the gage has a high gage factor of about 80. This result is shown in Fig 6b. As shown in this figure, the poor

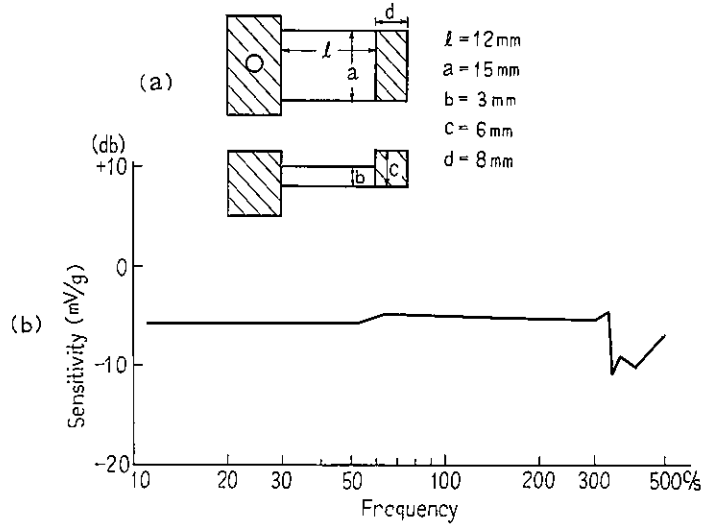


Fig. 6. Frequency characteristics of sensitivity of accelerometer with semiconductor strain gage and of which theoretical resonance frequency is 2.85 kc.

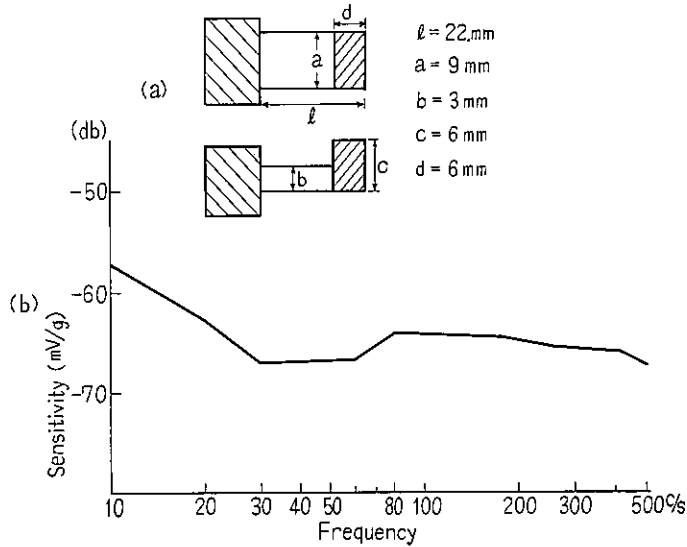


Fig. 7. Frequency characteristics of sensitivity of the same type accelerometer as that of Fig (6), but having common wire strain gage and of which theoretical resonance frequency is 2.025 kc.

EXPERIMENTAL STUDY ON APPLICATION OF STRAIN GAGE TO ACCELEROMETER

flatness of the curve found in the frequency range of over 300 c/s may be caused by the condition of cementing of the gage, the kind of adhesive and characteristics of clamping end of the cantilever beam as the accelerometer. However, considerable satisfactory result was obtained in the range of low frequency. In Fig 7a, the same cantilever accelerometer having common wire strain gage is shown. Comparing the curve of Fig. 7b with that of Fig. 6b, the excellency of the accelerometer with the semiconductor strain gage is proved clearly, as the sensitivity of accelerometer shown in Fig. 7b is 60 db lower than that of Fig. 6b.

AMPLIFIER TO DRIVE STRAIN GAGE

In order to measure the acceleration of vibrating tools in field research, a new amplifier for the strain gage was constructed. The amplifier is desired to have a property to satisfy the following conditions. (1) The frequency characteristics of amplifier is flat from 0 to 200 c/s. (2) Gain of the amplifier is variable enough to measure the acceleration from 1g to 200 g. (3) Out put of the amplifier can be recorded in the frequency ranged from 0 to 200 c/s by the tape recoder and the acceleration between 5~200 c/s can be known by reading the levelmeter, which is included in the amplifier. (4) The amplifier must be a small sized and portable one.

To meet these purposes, the amplifier was constructed by making use of transistors. The block diagram of the circuit and the actual circuit are shown in Fig. 8 and 9 respectively. The sine wave of the frequency 2000 c/s which is generated from the piezo electric fork oscillator, is amplified separately by means of each power amplifier.

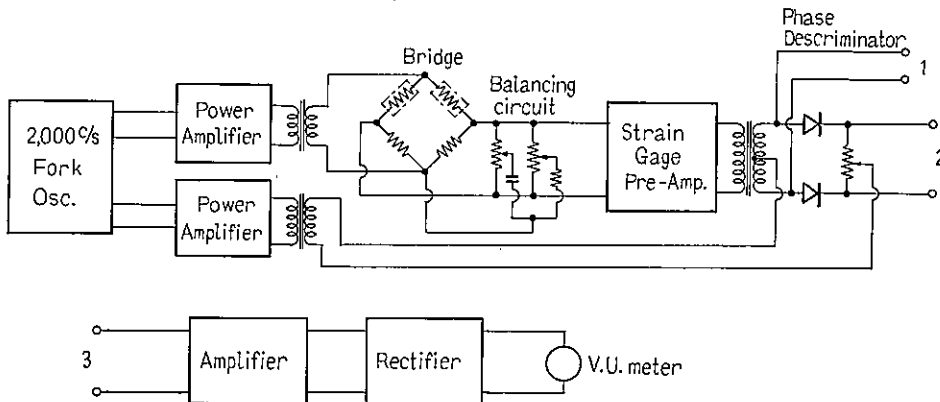


Fig. 8. Block diagram of circuit to drive strain gage.

The gain of the strain gage pre-amplifier is over 80 db. The out put 1 is made to check the bridge-balance. In this checking, out put 1 is connected with 3. In order to record the vibration with tape recorder, the out put 2 is used. To read the acceleration amplitude with meter, the out put 2 is connected with 3. V.U. meter has been calibrated by the acceleration with unit g.

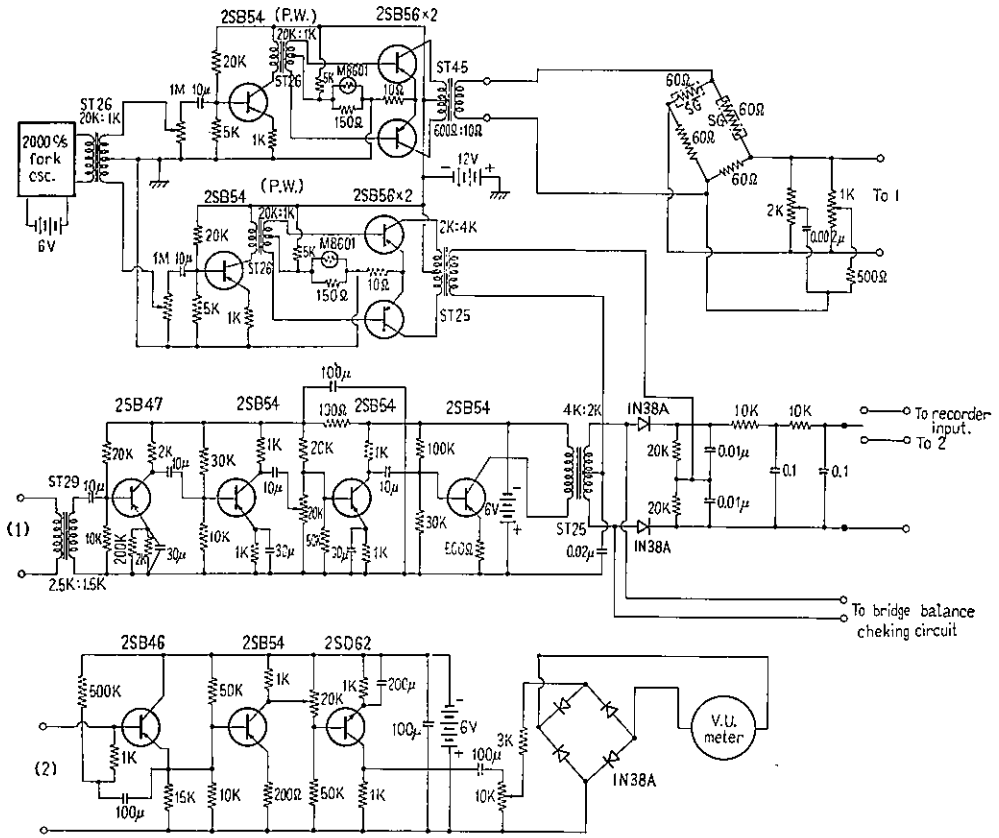


Fig. 9. Actual circuit to drive strain gage.

The out put of the one power amplifier is fed into a bridge and the out put of this bridge is amplified in the pre-amplifier. Then, both signals, which come from the out put of the other power amplifier and from the out put of the pre-amplifier of the bridge, are mixed in the phase discrimination circuit. The reason why 2000 c/s was chosen is to obtain ten times the frequency of the expected maximum frequency during the measurement of acceleration. After the accelerometer having the semiconductor strain gage was connected with this electric circuit, the instrument was calibrated by the shake table maintaining the acceleration of 1 g. As shown in Fig 10, this system can satisfy above conditions.

Finally a word must be said about the following items, which have been left to be solved in the future.

- (1) D.C. volt. of the semiconductor gage drifts with change of ambient temperatures. The circuit must be constructed so as to be compensated with this change of the D. C. voltage.
- (2) Further study must be undertaken how to calibrate the acceleration over 50 g.

EXPERIMENTAL STUDY ON APPLICATION OF STRAIN GAGE TO ACCELEROMETER

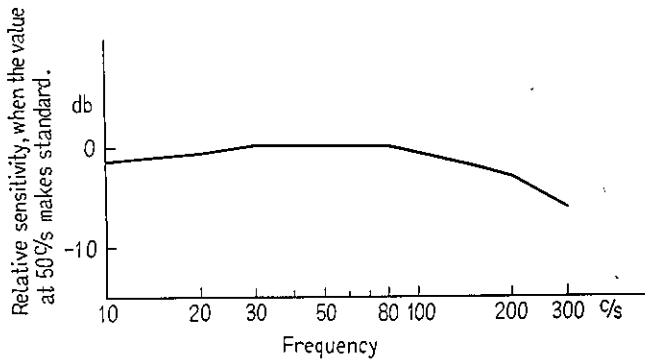


Fig. 10. Frequency characteristics of sensitivity of the instrument, in which accelerometer is connected with circuit described above, maintaining the acceleration amplitude of the shake table constant 1 g.

ACKNOWLEDGEMENT

I am grateful for the many ingenious ideas that were offered by Dr. J. Igarashi, Professor of Tokyo University and I should like to thank Dr. H. Sakabe for encouraging me to continue this study.

REFERENCES

- 1) Miura T.: J. Sci. Lab. Jap. **37**, 143, (1961).
- 2) Den Hartog J.P.: Mechanical Vibration. McGraw-Hill & Co., (1956).
- 3) Jacobsen L. S. and Ayre R. S.: Engineering Vibration with Application to Structures and Machinery. McGraw-Hill & Co., (1958).
- 4) Dobie W.B. and Issac C.G.: Electric Resistance Strain Gauges. English Univ. Press. (1953). Translated in Jap. By Miyake and Kato: Maruzen Co. (1958).
- 5) Yarnell J.: Resistance Strain Gauges Their Construction and Use, Offices of Electronic Engineering London (1951). Translated by Kawaguchi & Nagakura: Korona Co., (1960).
- 6) Harris C.M. and Crede C.E.: Shock and Vibration Handbook. Vol. 1, McGraw-Hill & Co. (1961).

要 旨

半導体ストレインゲージの加速度計への応用

三 輪 俊 輔

近時労働衛生の分野に於て、振動工具の生体への影響が大きな問題になっている。その影響を究明するには先ず、振動を正確に測る事から始める必要がある。しかし振動測定には次の問題が提起される。

(1) 振動対象への接着が強固か否か、(2) 振動ベクトルの主成分をえらんでいる否か、(3) 振動計の質量が、振動系に対して十分小さいか否か。

此の問題に解決を与えたものが、チタバリ振動計である。しかしこの振動計で低周波の振動を測定するには、高度の high input impedance 特性をもつプリアンプを必要とする。又此の振動計は静的変位に感じない。そこで著者は振動測定の為にこの欠点がなく、且上述3項の問題を解決出来る様な、半導体ストレンゲージをはった片持バリ式加速度計を試作した。

設計図及び此の加速度計の感度は第 6a 及び第 6b 図に示した。即ちこの図よりすぐれた感度特性をもつ事がわかる。但しこゝに感度とは本文の方程式 (7) より求められたものである。半導体ストレンゲージを用いた理由は感度がよい為である。ちなみに同じ片持バリ式加速度計に普通のワイヤーストレンゲージをはった場合、感度を求めると第 7a 図及び第 7b 図のようになる。即ち感度は後者の方が 60 db もわるい事がわかる。但し此の片持バリでは、普通のゲージも半導体ゲージでも 1 kc 以上になると感度がおちる。何故ならば、この片持バリの振動は 1 kc 以上では、その腕の振幅が小さすぎて、ストレンゲージでは感じない為である。

次に此の加速度計の現場使用を考えて下記の仕様により、トランジスタ増幅器を試作した。

- (1) 0~200 c/s 以内の振動加速度が測れる事
- (2) 感度は 1 g~200 g 程度の加速度が測れる事
- (3) 小型軽量である事
- (4) 0~200 c/s の範囲で録音器への入力が見られ、5~200 c/s ではメーターで加速度がよめる事

此の為のブロックダイアグラム及び実際の回路は第 8 及び第 9 図に示した。

此のアンプと上述の加速度計を結合して、相対感度を求めた所第 10 図の結果をえた。この図に示す様に、200 c/s でも相対感度は -3 db であるから、振動周波数が 0~200 c/s であれば、振動は測定可能である事を知った。

B. G. M. を効果的にする為の騒音対策

三輪 俊輔 野崎 互右

NOISE CONTROL TO FACILITATE HEARING OF BACK GROUND MUSIC IN AN ELECTRIC PARTS FACTORY

Toshisuke MIWA and Kosuke NOZAKI

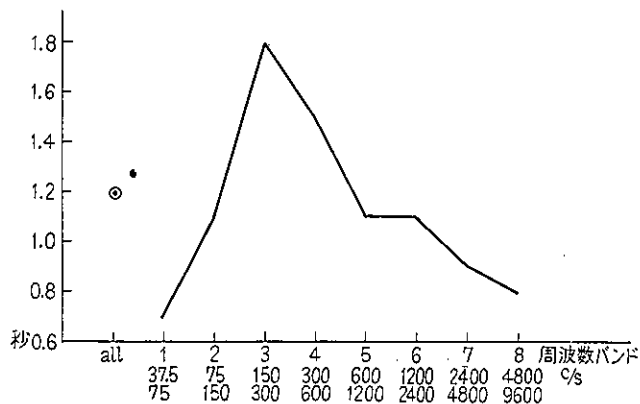
近代工場では工員一人が作業工程の多くの部分を受け持つ事は殆んどなく、流れ作業による場合が多い。この為、能率の問題が考えられる様になった。即ち採光、換気、騒音等を規正する事は勿論であるが、作業の単調化にともなう能率低下をさける為に B. G. M.¹⁾ (back ground music) の問題が取り上げられて来ている。此の為には室内の騒音は 80db 以下でなければ効果的でない。

今回某電気部品製造工場で、B. G. M. を行う為に、騒音を 80 db 以下にさげる様に依頼されたので、以下の測定を行い、且音響対策をした処、やゝ満足すべき結果をえたのでここに報告する。

§1 残響時間の測定

工場室内の音響特性はピストル音法²⁾で残響時間を測って求めた。

室の大きさは 400 坪、平均の高さ 7m、天井はシャーレン型でこの室は二階に位置している。即ちスタート用ピストル音を録音器で録音し再生しバンドパスフィルターで分析し、プルーエルのレベルレコーダーで記録し、その波形より残響時間を求めた。録音は中央の位置で行い、ピストル音は室の三点で発射した。此の平均値を第1図に示す。又 room constant³⁾を求めて見ると、 $R=1470$ で非常に自由音場に近い事が判った。



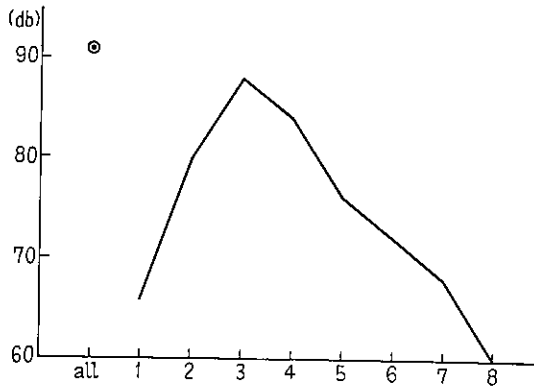
第1図 残響時間

§2 騒音の分析とその対策

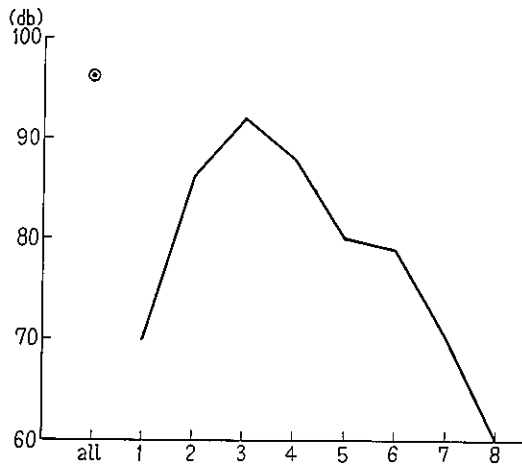
騒音源は室中に一様に分布しているが、主音源と考えられるものは、排気用のモーター類、これ等モーター類より配管されているダクトより発生する音、及び之等モーターの振動による2階の床、周囲の壁の共鳴の為に発生する音等であると考えられた。之等のレベル及びスペクトルは第2～4図に示した。

次に之等の主騒音源の対策として次の事項を行った。部分騒音源はすぐそばではかっても80フォン以下であったので今回はこの部分の対策は行わなかった。

- (i) 天井裏の2ヶのモーターは室外に出した。
 - (ii) 他の排気用モーター類は全体をブロックで囲みモーターの下には防振ゴムを敷いた。
 - (iii) ダクトとモーターの接続部及び各曲り部分に帆布のダクトを入れた。
- (音響測器の使用を指示したが、工場側の予算の関係で行われなかった。)

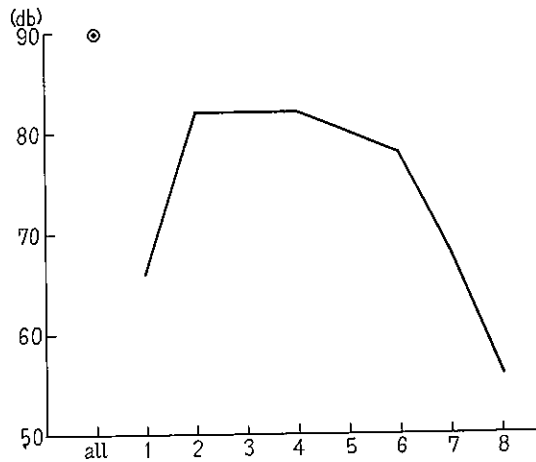


第2図 モーター音のスペクトル



第3図 ダクトの吸入口より発生する音のスペクトル

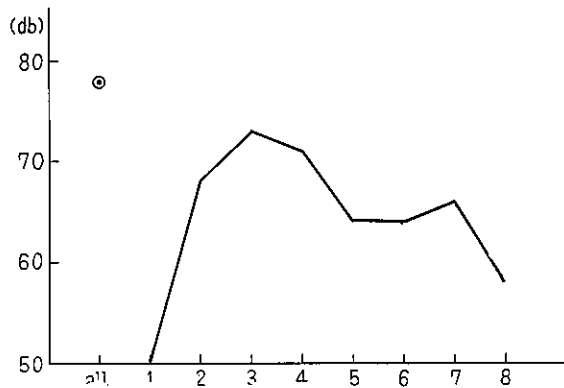
B.M.G. を効果的にする為の騒音対策



第4図 モーターの振動により発生すると思われる音のスペクトル

§3 結果

上述の様に処理した後騒音の平均レベルは 80 db 以下となり、殆んど音場は平均化された (第5図)。即ち処理前 105~85 フォンの騒音場も 78~80 フォンにさがった。故に B.G.M. を実施してよい状態になったものと思う。



第5図 処理後に於ける室内3点の平均スペクトル

文 献

- 1) Harris C. M. Handbook of Noise Control, Chapter 10. Effect of noise behavior, McGraw-Hill, (1957).
- 2) 五十嵐寿一: 日本音響学会誌 10, (4), 230, (1954), 12, (2), 55, (1956).
- 3) Beranek L.L.: Acoustics, McGraw-Hill, (1950).

防毒マスクの性能検査について—吸収罐除毒能力検査
の為の装置の作製

松村 芳美 興 重 治 左右田礼典 大 島 茂

THE TESTS FOR GAS MASKS.—APPARATUS FOR THE
DETERMINATION OF THE SERVICE LIFE OF CANISTERS

Yoshimi MATSUMURA, Shigeji KOSHI, Reisuke SODA
and Shigeru OSHIMA

For the determination of the service life of canisters, a new apparatus was designed and constructed and it was proved to be useful for the official approval of gas masks. The apparatus is equipped to carry out the examination in such an ambient condition as provided in JIS B-9903 (1955). In current JIS, it is described that the canisters are to be examined in such an air stream as being 30 l/min. in its velocity, at 20°C of temperature, 50 per cent of relative humidity and containing a certain concentration of a test gas. Besides, the leak gas concentration of the air which has passed through the canister, is to be determined with a sensitive test paper.

The new apparatus is equipped with the following functional parts: air stream generator, temperature and humidity controller, gas mixer, thermostated air bath for canister supporting and, at the last of the series, leak gas sampler. To observe the change of the leak gas concentration in the course of gas flow, a titration method was adopted at the same time with the test paper method.

Employing the apparatus, some canisters for sulfur dioxide were tested. In this case, the leak gas concentration was determined according to Thomas' method, in which gas was fractionally sampled in hydrogen peroxide solution and titrated with borax solution. As a test paper, litmus paper was used. Leak gas concentration-time curves of these canisters are reported.

防毒マスクの国家検定は、当研究所の業務の一つである。本論文では、マスクの種々の性能を JIS (B-第 9903 号, 1955 年) に定められている条件で検査する方法と装置を確立することを目的とした。マスクの性能としては、気密性、排気弁の作動機密性、通気抵抗、除毒能力があり、

THE TESTS FOR GAS MASKS

夫々についての標準値が JIS に於て明示されている。これらのうち、今回は除毒能力のみについて検査方法を確立し、作製した装置を用いて市販の亜硫酸ガス用吸収缶を対象として漏洩ガス濃度の測定を行った。漏洩ガス濃度測定には、試験紙法と並んで滴定法を用いた。滴定法は、漏洩ガスを捕集瓶を用いて捕集液に溶解捕集した後、滴定によって定量する方法である。この方法は、破過点検知及び漏洩ガス濃度の時間変化を追跡するに当って、試験紙法より精度が高く、より適していることが明らかになった。

I 検査条件

吸収缶除毒能力の検査条件は、実際にそれが使用される時の環境空気の状態に近いことが必要であるが、JIS ではこれを標準化して次の様に定めている。即ち、吸収缶を通過する空気流は温度 20°C、相対湿度 50% (水蒸気分圧 8.77 mmHg) で、流速は毎分 30 l とする。この空気流に、吸収缶の種類によって定められた一種類のガスを、缶の大きさに応じて一定濃度に混合し吸収缶通過後に漏洩して来るガス濃度を測定する。最大許容漏洩限度に達する迄の時間が、JIS の破過時間より長ければ、その吸収缶は認可されることになる。例えば、亜硫酸ガス用の直結式吸収缶では、試験ガスとして亜硫酸ガスを空気流中に 0.3% 含有させ、15 分以内に、漏洩ガス濃度が 10 ppm に達するか否かを、感度 10 ppm 以下の試験紙で検知することとされている。

以上の条件を実現する為に、我々は次の様な一連の装置を試作した。

II 装置の構造と調整

装置は第 1 図の様な六つの部分から構成されている。即ち、空気流発生用コンプレッサーから、毎分 30 l の空気流を得、これに充分な (水蒸気分圧 8.77 mmHg 以上) 湿度を与えた後、温湿度調整装置で過剰な水蒸気を凝縮して除き、空気流温度を調節する。試験ガスがポンペで得られる場合には、そのガス取り出し口とロータメーターを直列に連結し、ガスの流速を測定してガス混合装置に導入し、空気流と混合する。こうして得た試験空気流を、20°C の恒温空気浴中に保持された吸収缶に導き、缶通過後の空気流の一部を漏洩ガス濃度捕集装置に通し、残りの部分は排気した。以上のうち、第 1 図の 6～8 の部分は、有害ガスが漏れる恐れがある為、ドラフトの中に設置してある。

各部分の駆動状況は次の様である。

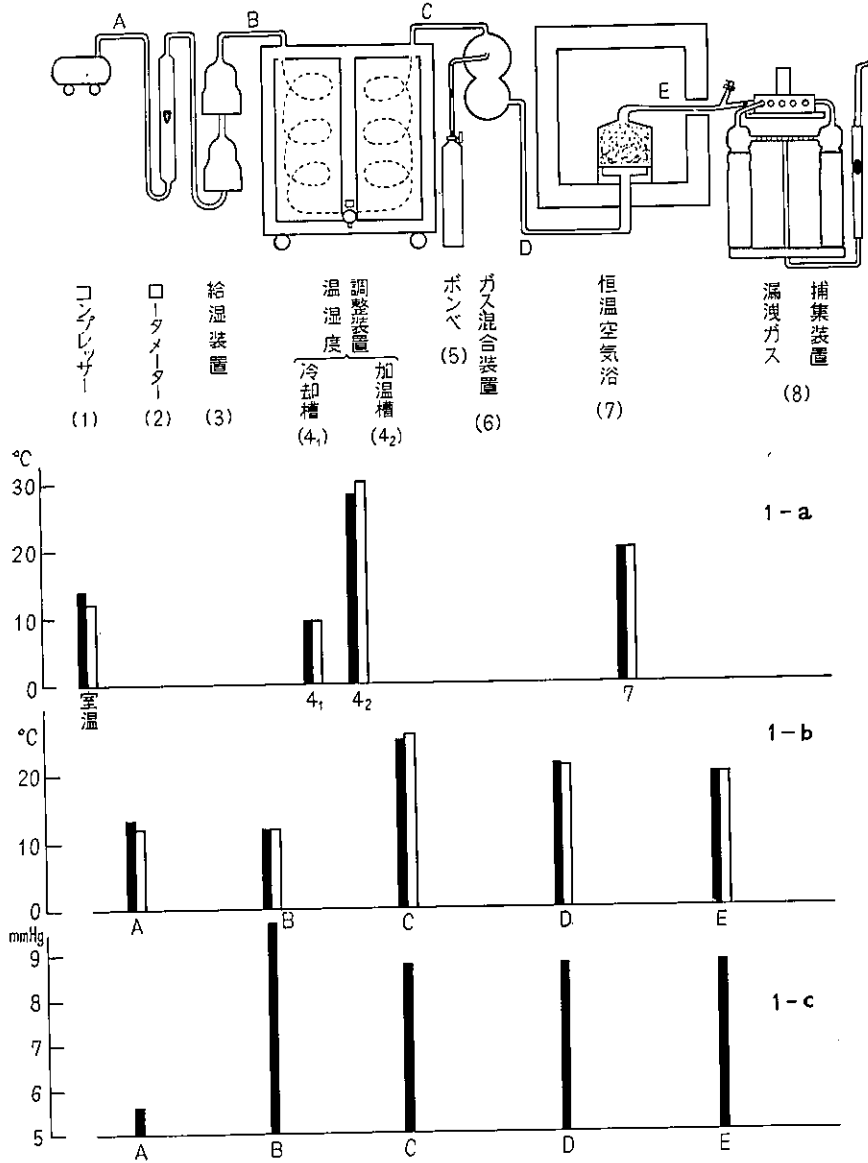
コンプレッサー

最高圧力 10 kg/cm²、圧力振幅 1.5 kg/cm² の容量 50 l のものを用い、これに二段減圧バルブ及び抵抗を入れて流速の脈動を小さくした。流速 30±1.5 l/min の空気流を得ることが出来た。

給湿装置

夏期には、大気が多湿である為、この装置は殆んど必要ないが、冬期には、大気中の湿度分圧が 8.77 mmHg 以下になるので、湿度を与える必要がある。

給湿装置としては、水を満した Dautreband インピンジャー二個を直列に連結したものを用いた。給湿後の空気流の湿度は、検定附二重ガラス管の気象用温度計を用いた乾湿球で線速度 3 m/sec の空気流中で測定した。給湿の期間中は、ヒーターでこれら装置を加温し、装置内の水温が、水の気化によって低下して、給湿効率が下ることを防いだ。この様にして、空気流の相対湿度は 12～15°C で 92～95% に調整され、目的を達することが出来た。



第 1 図

装置のフローダイアグラムと作動状態：(1-a) 装置各部 (1~8) の温度，(1-b) 空気流の各位置 (A~E) での温度，(1-c) 空気流の各位置 (A~E) での湿度，□は室温 12°C の時，■は室温 14°C の時の装置各部及び空気流の温度を示す。

ガス混合装置

試験ガスがポンペで得られる場合には，直接ポンペの減圧バルブとロータメーターを連結し，ガス混合装置に導いた。ガス混合装置は，試験ガスと空気流が均一に混合される様に，乱流の多

THE TESTS FOR GAS MASKS

い状態にし、且、空気の線速度を落して静圧を安定させ、ここにキャピラリーを通じてガスを導入した。この様にして、コンプレッサーから発生する空気流量の脈動による、ガス流入量及びロータメーターの検量の変動をなくし、安定に混合することが出来た。試験ガスがボンベで得られず、化学的に発生させる必要のある場合及び有機物の場合には、別の装置を考慮する必要がある。

温湿度調整装置

この装置は、温度の異なる二つの水槽と、夫々の水槽の温度制御系からなっている。給湿された空気流は先ず低温水槽で水蒸気分圧 8.77 mmHg の露点 9.37°C に冷却され、過剰な水蒸気はドレインとして除いてから、高温水槽中で適当な温度まで加温される。温湿度調整装置から吸収缶に達する迄の空気流路の壁の断熱が充分でない為、温湿度調整装置の高温水槽側では、空気流温度を冬期には 20°C より高く、夏期には 20°C より低い温度に調整する必要がある。尚、絶対湿度の流路に於ける損失はみられなかった。第 1 図に、装置の各部の調整温度と、それらを通過する時の空気流の温度、湿度を示した。

恒温空気浴

之は吸収缶を 20°C に保つための空気浴で、壁面は 20°C の循環水と炭化コルクの断熱材で囲まれている。20°C の水は、別の水温制御水槽から、ポンプで循環されている。恒温空気浴内の温度は一定で、殆んど変動はみられなかった。

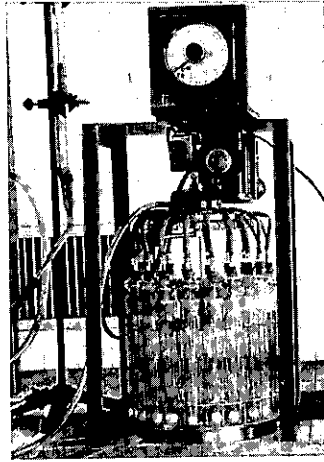
漏洩ガス捕集装置

試験紙法は、JIS に特記された方法なので、定められた破過限度の時間から 1 分間行い、漏洩ガス濃度が最大許容濃度の上下いづれであるかの検知を目的とした。滴定法は、吸収缶に試験空気流を流し始めた時から、漏洩ガス濃度の時間変化を追跡するのに用い、第 2 図に示した様な漏洩ガス捕集装置によった。この装置は、20 本の捕集瓶を設置する台と、15 分から 10 秒の間の任意の時間間隔で空気流路を切り換えることの出来るタイマーつきセレクターから成っており、各捕集瓶の中に、一定時間づつ、空気が採取される様になっている。ガス捕集瓶は、長いミゼットインピンジャー型の容器に、シスタードガラスのボールフィルターをバブラーとして用いたもので、捕集効率は殆んど 100% である。この中に捕集溶液を入れてガスを吸収し、捕集液について滴定した。ボールフィルターの通気抵抗が大きいため、この抵抗に抗して空気流 1 l/min を採気するには、空気流路全体に大きな静圧をかける必要があり、これは吸収缶のガス吸着能力の測定及び空気や混合ガスの正確な流量測定には好ましくない。それで、30 l/min の空気流の一部を捕集瓶中に採気するに当っては、空気流を一度大気圧下に流出させ、その一部を吸引ポンプで瓶中に導入した。又、捕集瓶が換ると、ボールフィルターの通気抵抗が変動するので、流路セレクターが移動する毎に、採気速度が 1 l/min になる様、流路に適当な抵抗を入れることによって調節した。試験紙法の場合は、試験紙をセルロイドの枠にはめたものを、同型のインピンジャー内に入れ、ボールフィルターの代わりにガラス管で空気流を内部に導入して、色の変化を観察した。空気流としては、滴定法の為に 1 l/min を採気した残りの 29 l/min を、1 分間インピンジャーに導入した。

Ⅲ 漏洩ガス濃度及び破過点の測定——亜硫酸ガス用直結式吸収缶について

1) 試験紙法

次の 6 種類の試験紙について、製法の難易、感度、精度について検討した。



第2図

- (a) マラカイトグリーンの変色
- (b) 水酸化ニッケルの酸化による緑色から黒への変色
- (c) ニトロプルシッド亜鉛の淡いピンクから淡紅色への変色
- (d) 沃素酸カリウム——沃化カリウム——澱粉紙の紫褐色への変色
- (e) 沃化カリウム——沃度——澱粉紙の脱色
- (f) リトマス試験紙の青色から淡紅色への変色

以上のうち、(a)、(b)及び(e)は製法が容易で反応も比較的安定であるが、感度が低かった。(b)及び(c)は、製造の過程に加熱や乾燥があり、これらの操作が感度に影響して、常に一定の感度のものが得難かった。(c)の感度は、10 ppmの亜硫酸ガスを含んだ空気に接触すると、わずかに変色が見られる程度であったが、上記の理由で採用しなかった。(f)として、市販のリトマス試験紙を水にぬらして用いると、約1 ppmで変色が認められたが、更に高濃度では、濃度と変色の対応が不明確であった。又、変色程度は空気中に放置することより容易に変化した。試験紙をぬれた状態で使用するの、これと同じ状態の標準比色系列を作ることは困難であった。結局、試験紙法としては、リトマス試験紙を用い、変色から濃度を推定することは全く経験によった。

2) 滴定法

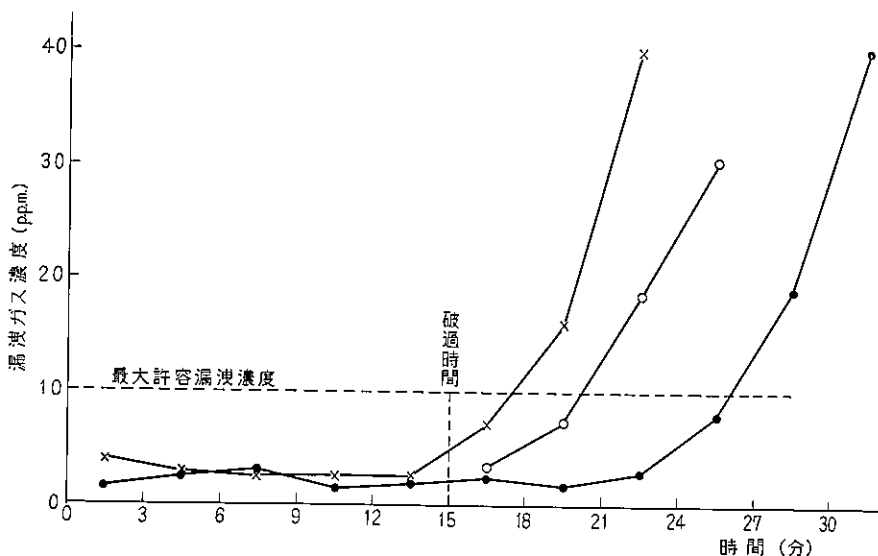
Thomas法によった。捕集溶液として0.003%の過酸化水素水溶液を用い、炭酸ガスの溶解による影響を防ぐために硫酸によってpH4.5~5.0に調整した。この溶液20 ccを捕集瓶に入れ、空気を1 l/minの流速で通気することにより、亜硫酸ガスを捕集、酸化し、捕集溶液は、捕集瓶の中でブロムクレゾールグリーンマラカイトグリーン混合指示薬0.2 ccを加え、N/250のBorax液で滴定した。

3) 結果

市販の直結式吸収缶を、恒温空気浴中に設置し、吸収缶全体が20°Cに保たれるのを待って、試験空気流を送った。漏洩ガスは、空気流を流し始めた時から3分間隔で流速1 l/minでインピンジャー内に分取し、滴定によって各採気期間の平均濃度を測定した。JISの規則に従って、

THE TESTS FOR GAS MASKS

試験ガスを流し始めた時から15分後に一分間、試験紙を用いた。結果の一部を第3図に示した。



第3図 吸収缶漏洩ガス濃度の時間変化
市販の亜硫酸ガス用直結式吸収缶について

以上の装置は、二つの温度の異なる水槽を用いて、空気流の温湿度調整を行っているのが特徴である。即ち、空気流を、目的とする水蒸気圧の露点まで冷却した後、適当な温度まで加温するのである。しかし、装置の各部分を連絡する空気流路の断熱が不完全である為、この部分で、外部の気温によって、空気流の温度変化が生じる欠点がある。又、コンプレッサーを空気流発生に用いている為、空気の流量に脈動が生じること、空気流路の各部に、測定時に使用した試験ガスが溜り、又は管壁に附着して、これの排気が不完全な場合には次の測定にそれらガスが流出して来る恐れがあること等の欠点があるので、逐次改良を加える必要がある。

文 献

- 1) Feigl, F.: Spot Test I. Inorganic Applications. Elsevier Publishing Co. (1954).
- 2) Koshi, S and Sakabe, H.: Bulletin of the Institute of Public Health (Tokyo), **66**, 25, (1957).
- 3) Jacobs, M.B.: The Analytical chemistry of Industrial Poisons, Hazards and Solvent. Interscience Publishers Co., (1949).
- 4) Allen, J.R., Walker, J.H. and James, J.W.: Heating and Air conditioning. McGraw-Hill Book Co., (1946).
- 5) McClaim, C: Fluid Flow in Pipes. The Industrial Press, (1952).

労働省労働衛生研究所研究報告

第六号

昭和36年

内容目次

トルエン中毒の実験的研究及びベンゼン中毒の回復過程に及ぼす

トルエンの影響について……………長谷川弘道 佐藤 光男…(1)

種々鉱物性粉じんのラット腹腔内単核細胞に対する影響について

……………奥 貴美子 林 久人 浜田 晃 坂部 弘之…(10)

表面性状の異なる各種石英粉末の線維増殖能…坂部 弘之 梶田 昭 奥 貴美子…(28)

ミストの粒度の測定……………林 久人 奥 重治 坂部 弘之…(35)

半導体ストレンゲージの加速計への応用……………三輪 俊輔…(43)

B. G. M. を効果的にする為の騒音対策 ……三輪 俊輔 野崎 互右…(53)

防毒マスクの性能検査について——吸収罐除毒能力検査のための装置の作製

……………松村 芳美 奥 重治 左右田礼典 大島 茂…(56)

Bulletin
of
The National Institute of Industrial Health

CONTENTS

- H. HASEGAWA AND M. SATO:** Experimental Study on Toluene Poisoning and Effect of Toluene upon the Recovery from Benzene Poisoning in Rats (1)
- K. KOSHI, H. HAYASHI, A. HAMADA AND H. SAKABE:** The Toxic Effect of the Various Dusts on the Intraperitoneal Monocyte in Rat. (10)
- H. SAKABE, A. KAJITA AND K. KOSHI:** Fibrogenic Activity of Quartz of Different Surface Properties..... (28)
- H. HAYASHI, S. KOSHI AND H. SAKABE:** Determination of Mist Size by Metal Coated Glass Slide. (35)
- T. MIWA:** Experimental Study on Application of Strain Gage to Accelerometer. ... (43)
- T. MIWA AND K. NOZAKI:** Noise Control to Facilitate Hearing of Back Ground Music in an Electric Part Factory. (53)
- Y. MATSUMURA, S. KOSHI, R. SODA AND S. OSHIMA:** The Tests for Gas Masks. —Apparatus for the Determination of the Service Life of Canisters. ... (56)